Diapiri

Formazione di diapiri:

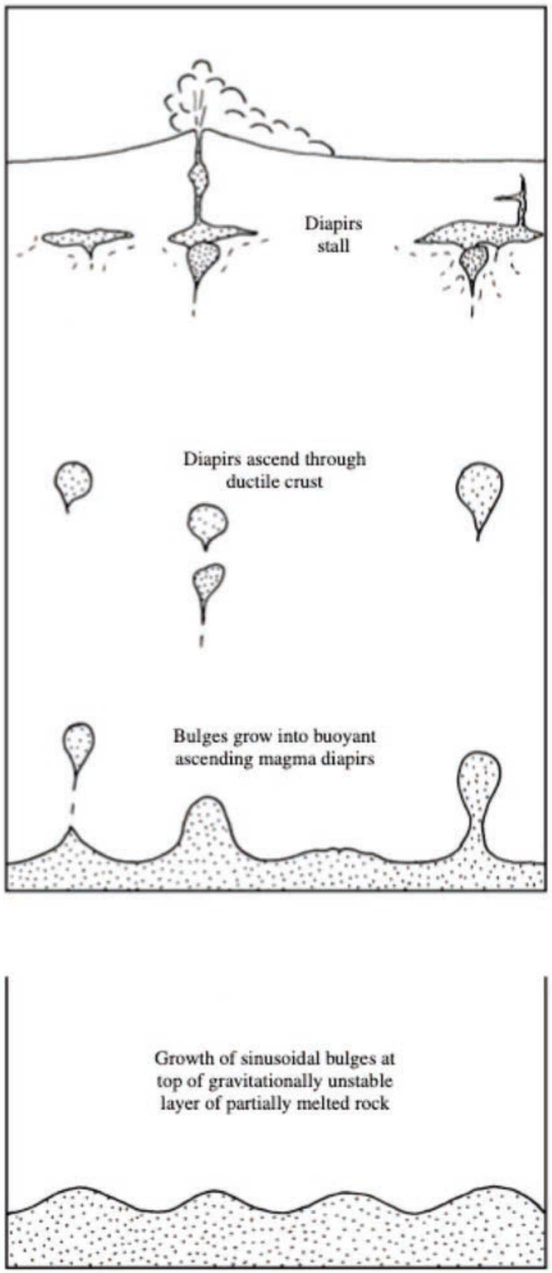

Best (2003)

I termini diapiri e *plumes* sono usati per indicare volumi di materiale che risalgono per effetto di un contrasto di densità con il materiale circostante, ovvero per «galleggiamento» (*buoyancy*).

Il termine plume è più utilizzato per volumi di mantello (*mantle plumes*), mentre il termine diapiro è utilizzato per contesti crostali o comunque litosferici (e.g. diapiri salini, diapiri di magma).

9.15 Highly schematic diagram (not to scale) showing the growth, ascent, and stalling of buoyant magma **diapirs.** Beginning at bottom of diagram, a layer of partially melted rock (magma) in source region in upper mantle or lower crust of lesser density than the overlying rock develops sinusoidal Rayleigh-Taylor instabilities. In next higher frame of diagram, these bulges grow and separate from the source layer, forming inverted "tear-drop"-shaped diapirs of magma that ascend through denser ductile country rock, as do hot-air balloons rising into the atmosphere. Eventually (top of diagram), magma diapirs stall at a density barrier or where they encounter stronger brittle rock. Subsequent diapirs may follow in the wake of earlier ones. Some magma may erupt.

Diapiri

Formazione di diapiri:

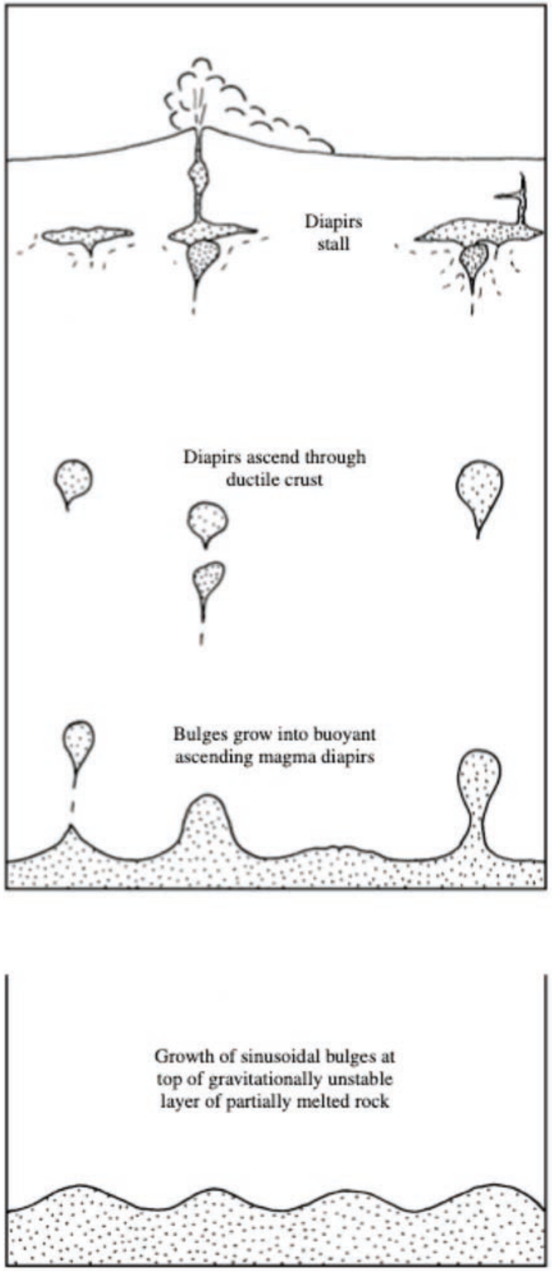

Il principio alla base della formazione dei diapiri è basato sul fatto che qualsiasi corpo di materiale poco denso che sta al di sotto di un corpo più denso è instabile dal punto di vista gravitazionale.

Nel caso i corpi siano tabulari e stratificati, la parte superiore del corpo meno denso tenderà a formare delle protuberanze sinusoidali, chiamate instabilità di Rayleight-Taylor, che cresceranno fino a quando l'inversione di densità viene stabilizzata.

9.15 Highly schematic diagram (not to scale) showing the growth, ascent, and stalling of buoyant magma **diapirs.** Beginning at bottom of diagram, a layer of partially melted rock (magma) in source region in upper mantle or lower crust of lesser density than the overlying rock develops sinusoidal Rayleigh-Taylor instabilities. In next higher frame of diagram, these bulges grow and separate from the source layer, forming inverted "teardrop"-shaped diapirs of magma that ascend through denser ductile country rock, as do hot-air balloons rising into the atmosphere. Eventually (top of diagram), magma diapirs stall at a density barrier or where they encounter stronger brittle rock. Subsequent diapirs may follow in the wake of earlier ones. Some magma may erupt.

Best (2003)

Diapiri

Formazione di diapiri:

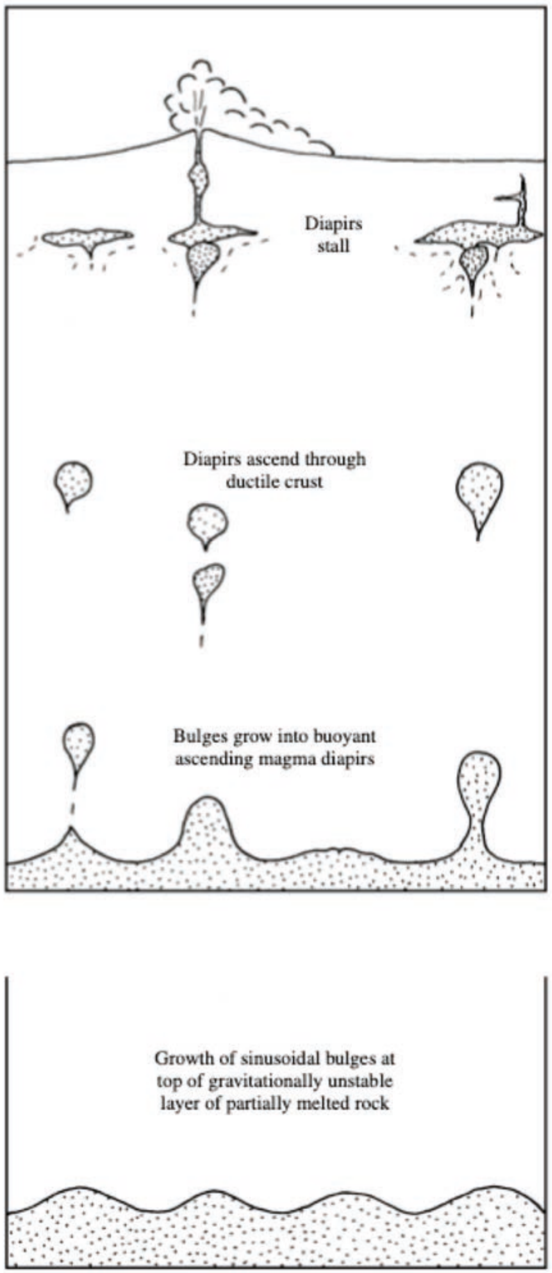

La velocità di risalita dei diapiri e la loro durata sono funzione di molti parametri, tra i quali le dimensioni e la forma dei diapiri stessi.
Maggiore sarà il rapporto tra volume e area del diapiro, maggiore sarà la forza di galleggiamento e minore sarà la resistenza alla trazione.
Quindi, la forma ottimale per un diapiro sarà quella di una sfera, che tra le altre cose, è anche quella che permette di avere una perdita di calore per conduzione inferiore.

9.15 Highly schematic diagram (not to scale) showing the growth, ascent, and stalling of buoyant magma **diapirs.** Beginning at bottom of diagram, a layer of partially melted rock (magma) in source region in upper mantle or lower crust of lesser density than the overlying rock develops sinusoidal Rayleigh-Taylor instabilities. In next higher frame of diagram, these bulges grow and separate from the source layer, forming inverted "tear-drop"-shaped diapirs of magma that ascend through denser ductile country rock, as do hot-air balloons rising into the atmosphere. Eventually (top of diagram), magma diapirs stall at a density barrier or where they encounter stronger brittle rock. Subsequent diapirs may follow in the wake of earlier ones. Some magma may erupt.

Best (2003)

I grandi corpi granitici affioranti oggi sulla superficie erano dei diapiri?

La formazione di un granito per diapirismo può essere provata solamente quando si può dimostrare che vi sia stata una risalita verticale del corpo viscoso

Mongolia centrale

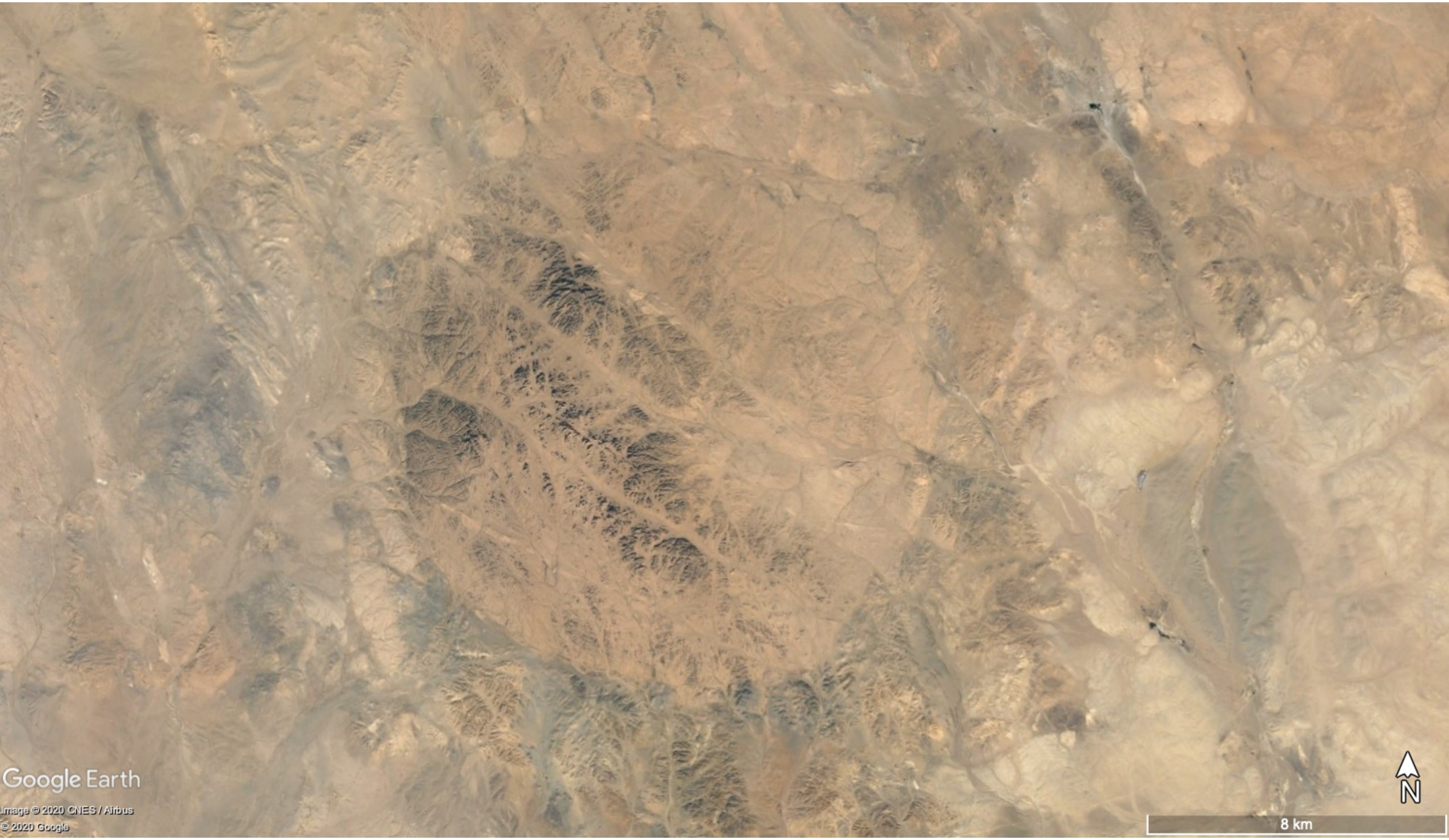

North Arran Granite Pluton (Scozia)

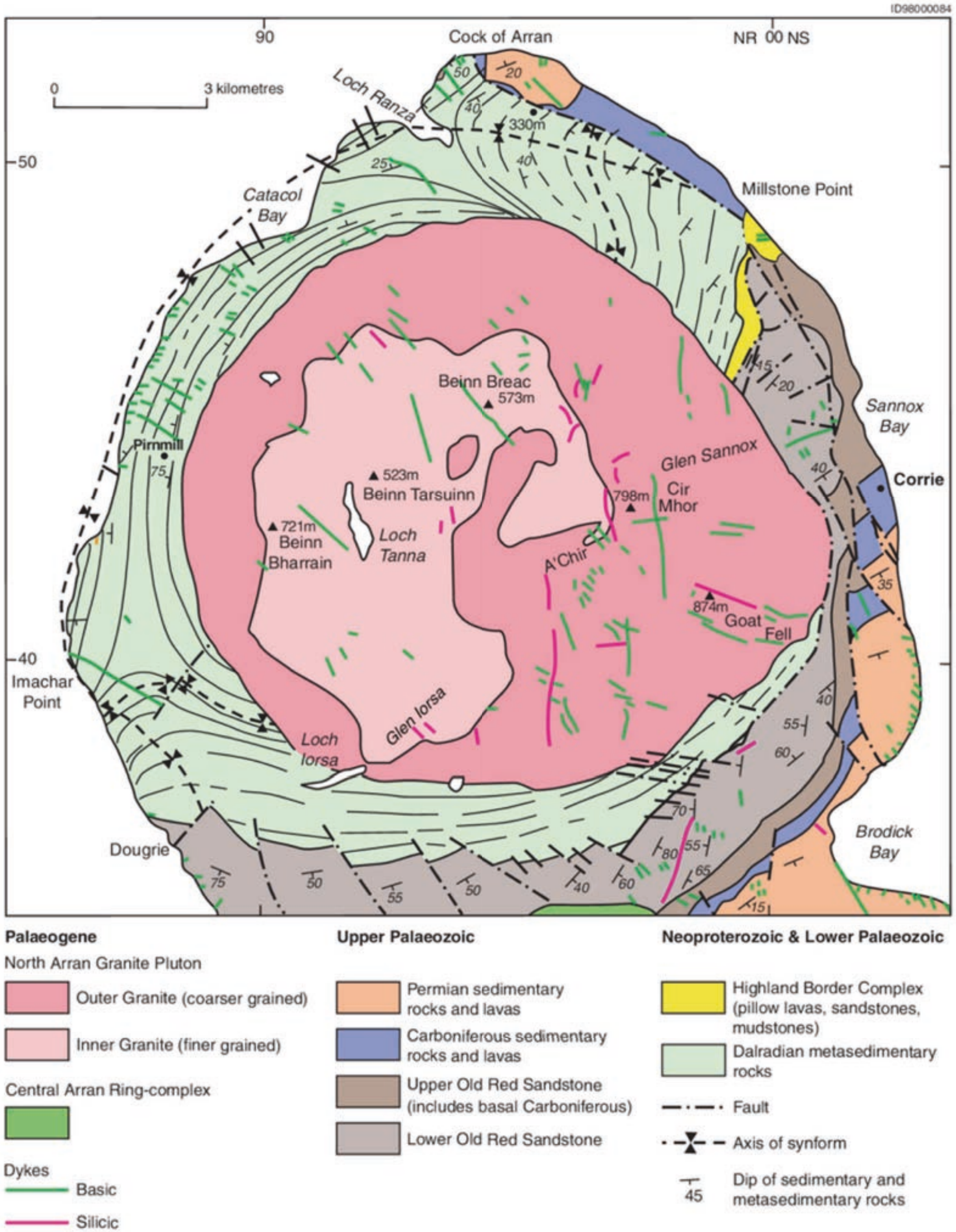

Emeleus & Bell (2005)

Isola d'Elba

Isola d’Elba

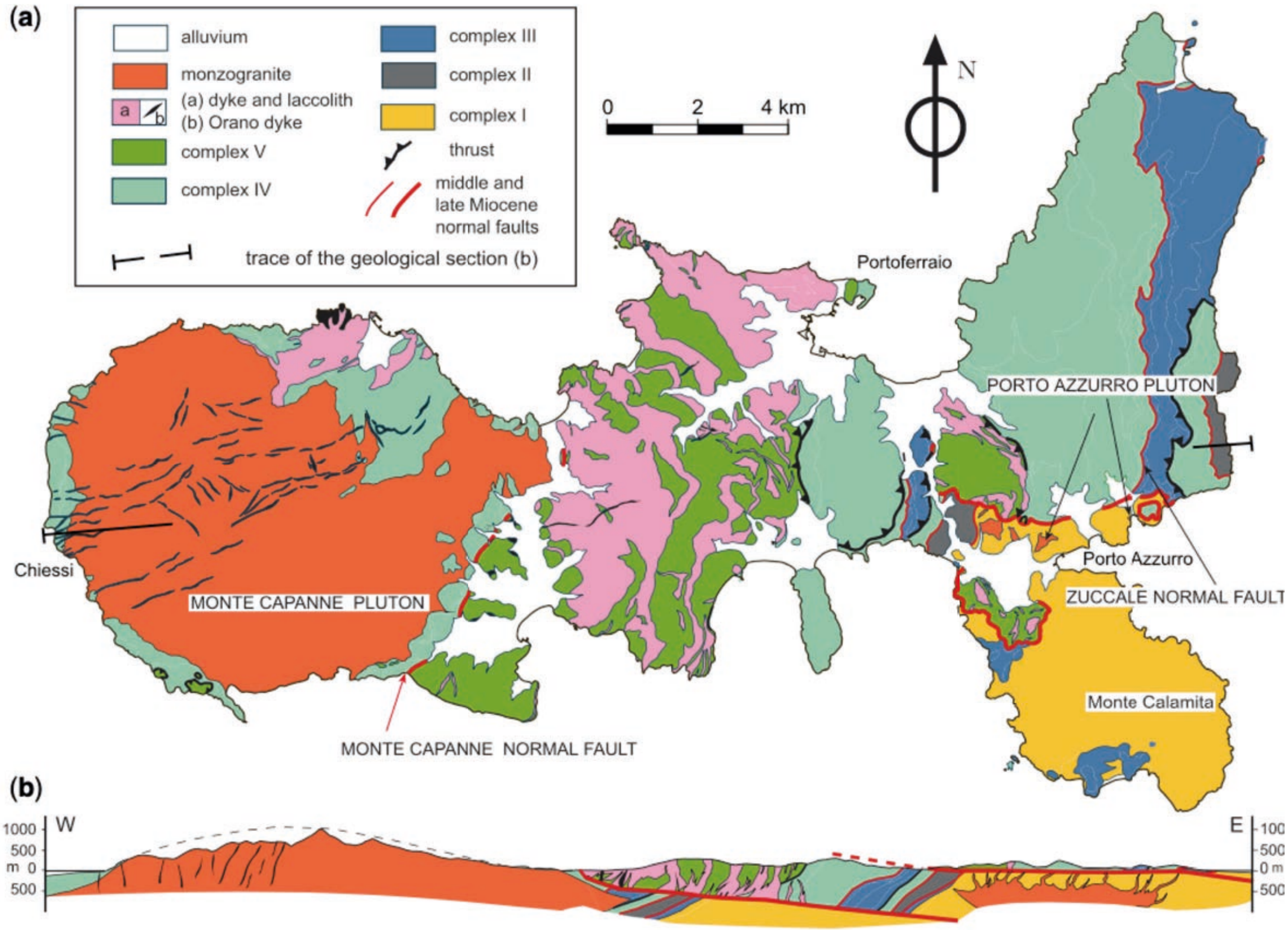

Fig. 2. Elba Island: (**a**) schematic geological map and (**b**) cross-section. The Monte Capanne pluton is exposed for *c.* 67 km^2.

Caggianelli et al (2015; Geol. Soc. London Spec. Publ.)

La messa in posto dei magmi nella crosta
(la formazione dei plutoni)

La messa in posto di un corpo magmatico al di sotto della superficie implica che un certo volume di crosta deve essere spostato.

Per quanto riguarda i magmi derivanti dal mantello, due sono i modi possibili tramite i quali un magma si fa spazio nella crosta per poter formare dei corpi plutonici:

1) tramite sollevamento della superficie
2) tramite inspessimento crostale, ossia il limite crosta-mantello (Moho) si abbassa, compensando il volume di mantello che ha fuso per creare il magma stesso

Lo spazio necessario per i magmi generati o derivanti dalla crosta inferiore può d’altra parte essere creato anche tramite movimento della porzione di crosta verso il basso.

La maggior parte delle intrusioni esposte oggi sulla superficie sono composizionalmente e tessituralmente eterogenei.

In base al tipo di eterogeneità, possiamo dividere le intrusioni in due tipi principali:

- **Intrusioni composite.** Sono composte da volumi composizionalmente e/o tessituralmente diverse che riflettono la messa in posto di due o più magmi ben distinti.

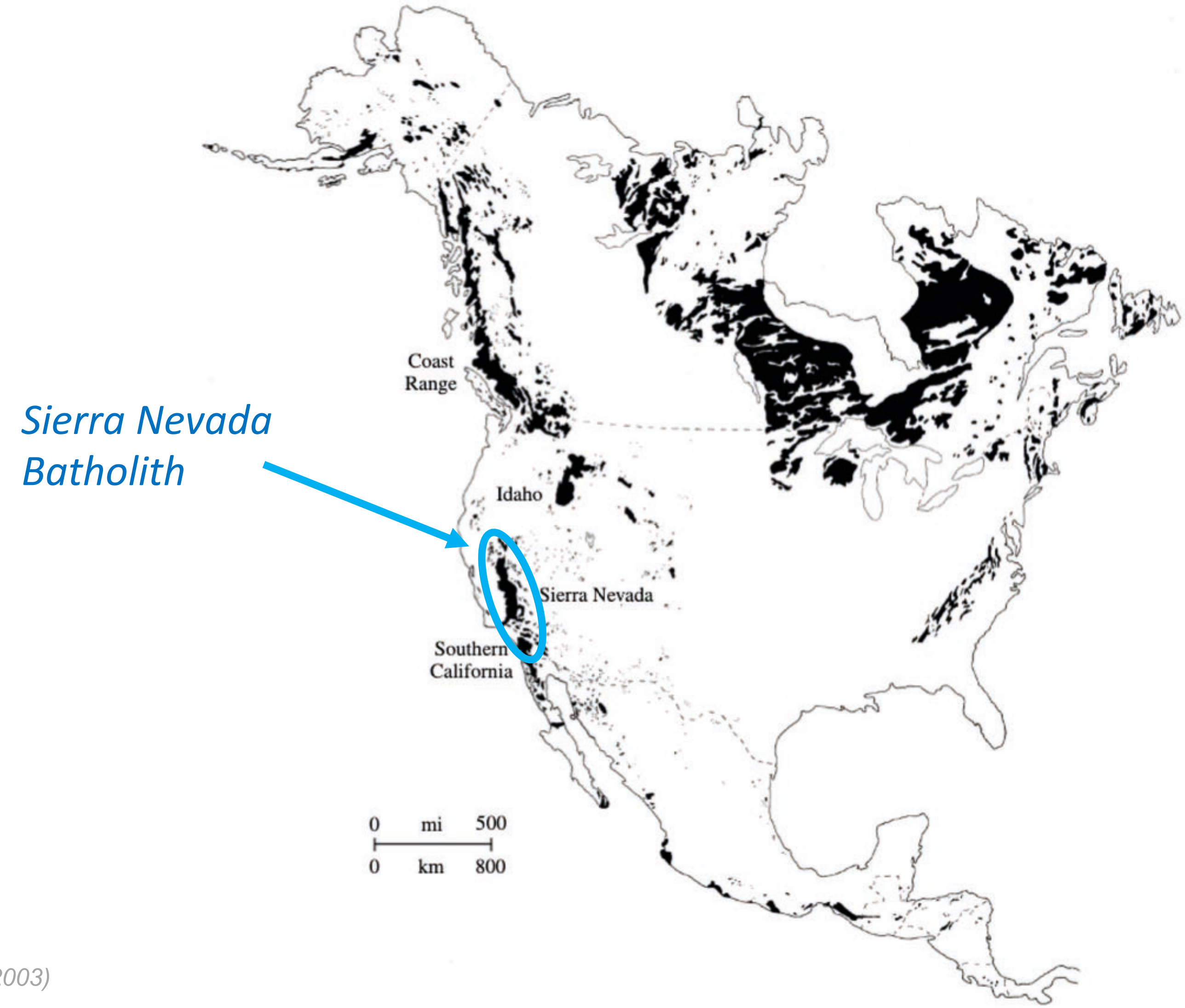

Best (2003)

9.16 Distribution of exposed granitic rocks in North America. Granitic rocks in Precambrian Canadian shield are generalized and include some metamorphic rocks. Rocks in the Appalachian orogen along the U.S. East Coast are mostly Paleozoic. Labeled **batholiths** along the west coast in the Cordilleran orogen are mostly Mesozoic. (Redrawn from the Tectonic Map of North America, U.S. Geological Survey.)

Sierra Nevada Batholith

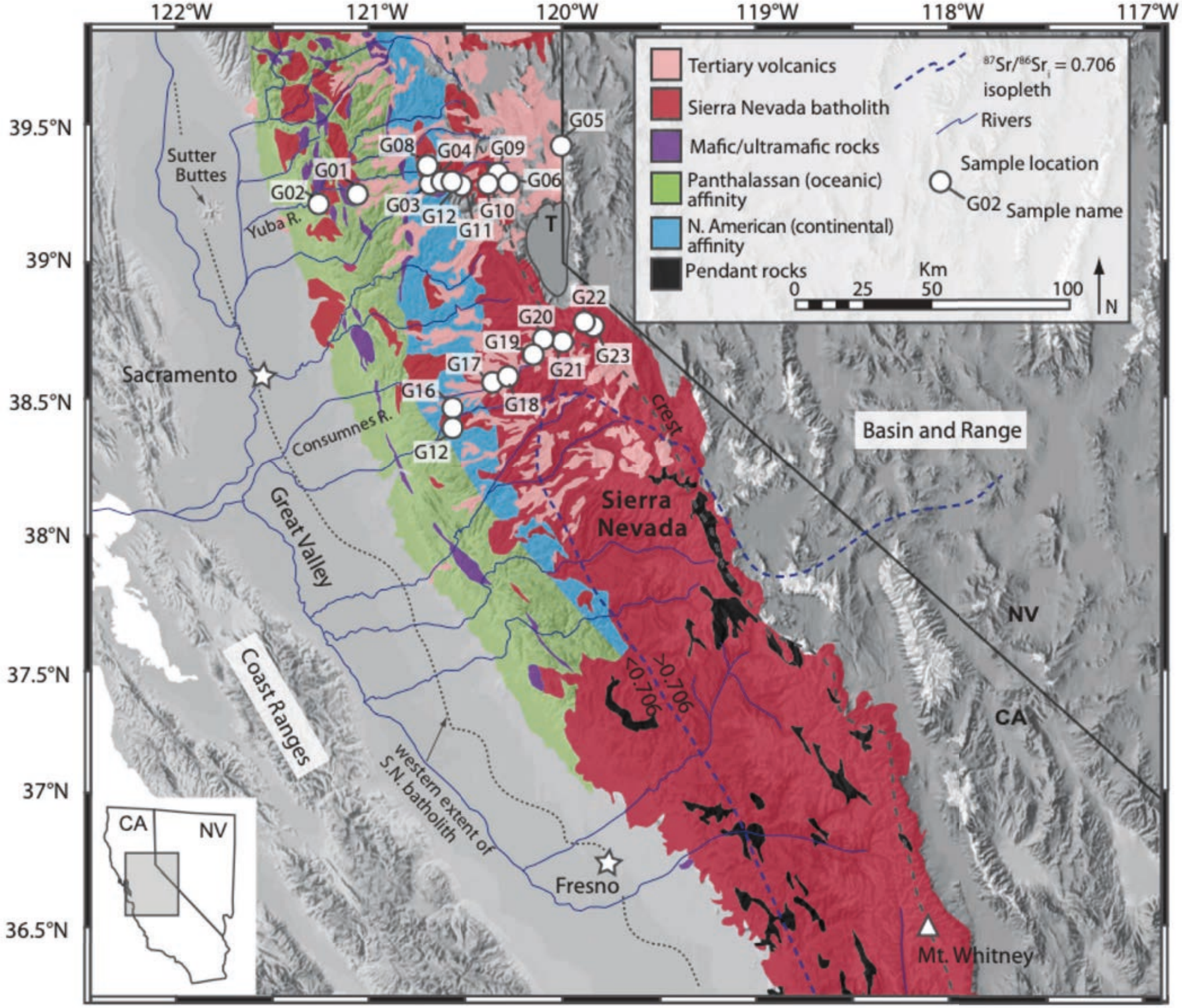

Figure 1. Generalized geologic map of the central and northern Sierra Nevada, modified after Irwin and Wooden (2001), Saucedo and Wagner (1992), and Wagner et al. (1987). Sample locations (and their corresponding names) are shown in white. The Sr_i 0.706 line is modified after Kistler and Peterman (1978) and Kistler (1990). Belts of metamorphic rocks in the northern Sierra foothills have been grouped according to the two different interpreted lithosphere types (Panthalassan and North American) of Kistler (1990). The western extent of the Great Valley is based on the presence of tonalitic and gabbroic arc-related basement sampled in well cores (Williams and Curtis, 1977; Saleeby, 2007).

Cecil et al. (2011; Geosphere)

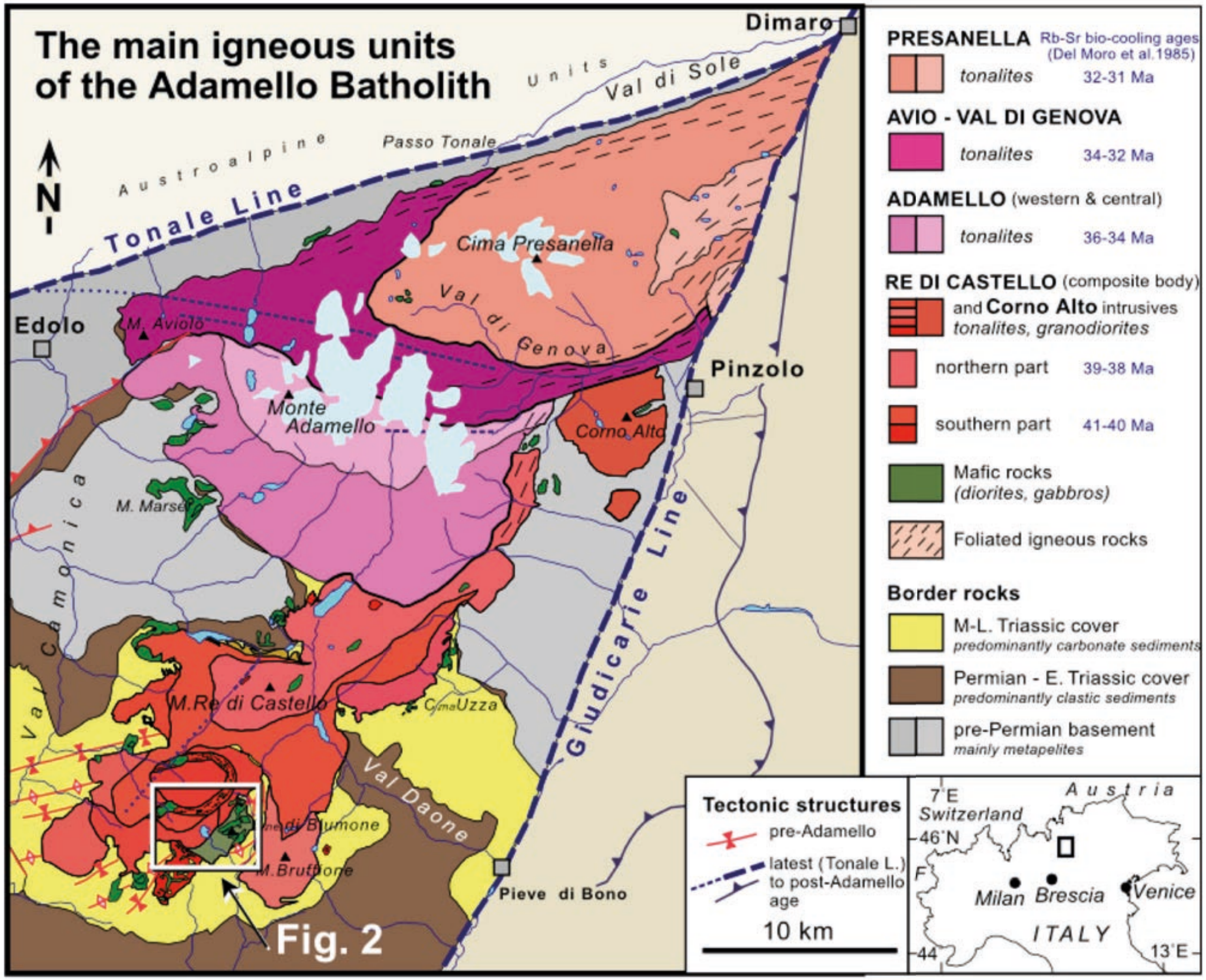

Fig. 1. Simplified geologic map of the Adamello batholith after Schaltegger et al. (2009), illustrating the approximate ages, lithologic characteristics, and designations of the main igneous units. See Schaltegger et al. (2009) for more detailed map and geochronology of the Re di Castello pluton. Location of the field site and Fig. 2 is outlined by the white box.

Schoene et al. (2012; EPSL)

La maggior parte delle intrusioni esposte oggi sulla superficie sono composizionalmente e tessituralmente eterogenei.

In base al tipo di eterogeneità, possiamo dividere le intrusioni in due tipi principali:

- **Intrusioni composite.** Sono composte da volumi composizionalmente e/o tessituralmente diverse che riflettono la messa in posto di due o più magmi ben distinti.

In molti casi, l'intervallo temporale tra la messa in posto dei vari magmi può essere anche grande, tale ad esempio da permettere la formazione di ***chilled margin*** in corrispondenza del contatto tra i due corpi. In altri casi, l'intervallo temporale è più piccolo e il magma successivo si può intrudere prima ancora che il magma precedente si sia raffreddato sotto la sua T di *solidus*, formando contatti tra i corpi che mostrano evidenze di contrasto termico meno accentuato.

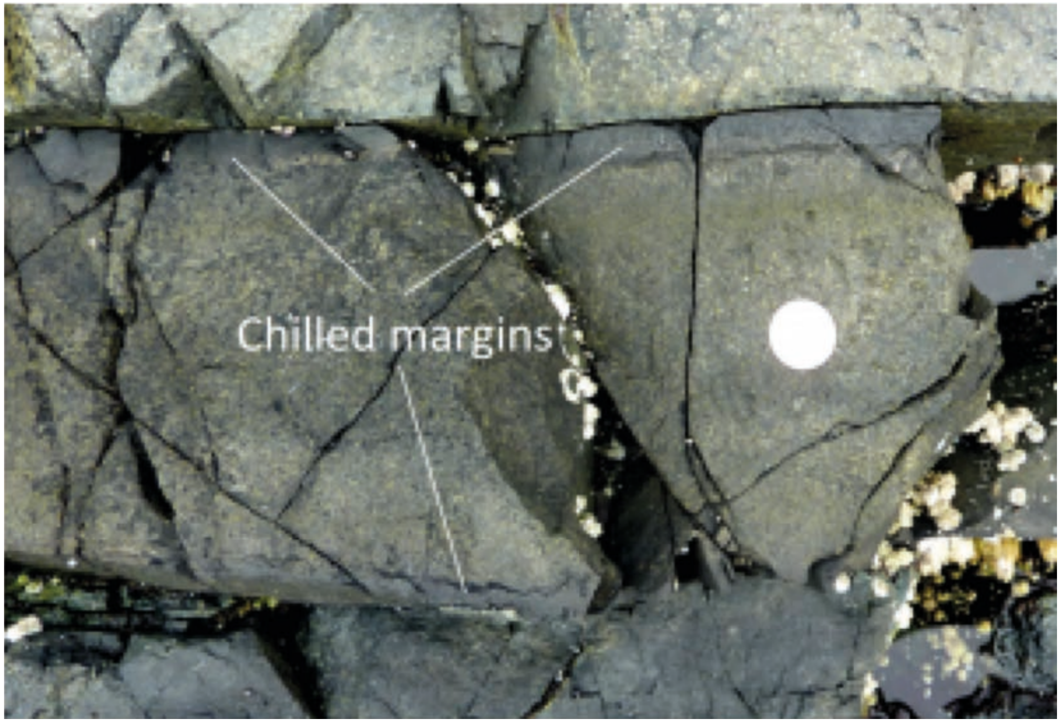

https://courses.lumenlearning.com/physicalgeology/chapter/3-5-intrusive-igneous-bodies/

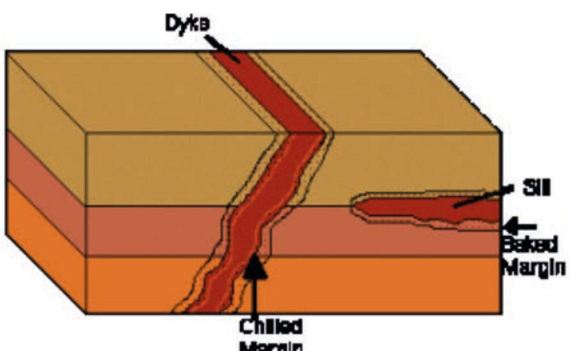

https://geologymike.wordpress.com/2013/10/21/rocks-made-by-fire/

La maggior parte delle intrusioni esposte oggi sulla superficie sono composizionalmente e tessituralmente eterogenei.

In base al tipo di eterogeneità, possiamo dividere le intrusioni in due tipi principali:

- **Intrusioni composite.** Sono composte da volumi composizionalmente e/o tessituralmente diverse che riflettono la messa in posto di due o più magmi ben distinti.
In molti casi, l'intervallo temporale tra la messa in posto dei vari magmi può essere anche grande, tale ad esempio da permettere la formazione di ***chilled margin*** in corrispondenza del contatto tra i due corpi. In altri casi, l'intervallo temporale è più piccolo e il magma successivo si può intrudere prima ancora che il magma precedente si sia raffreddato sotto la sua T di *solidus*, formando contatti tra i corpi che mostrano evidenze di contrasto termico meno accentuato.

- **Intrusioni zonate.** Esse sono invece composte da parti composizionalmente e tessituralmente diverse disposte in modo più o meno concentrico.
Nei plutoni con zonatura normale, queste parti sono sempre meno mafiche andando verso l'interno. Questo tipo di zonature si può sviluppare, ad esempio, per effetto di un diapiro di magma dioritico che si ferma ad un certo livello crostale e lungo la sua scia termica dei magmi più sialici e viscosi vanno a intrudersi al di sotto, flettendo verso l'alto il corpo dioritico. Alternativamente, una zonatura normale si può formare per assimilazione della rocca mafica incassante o tramite processi di cristallizzazione di un magma inizialmente omogeneo, nel quale i minerali mafici di più alta T cristallizzano preferenzialmente vicino ai margini.

Tuolumne batholith (Sierra Nevada)

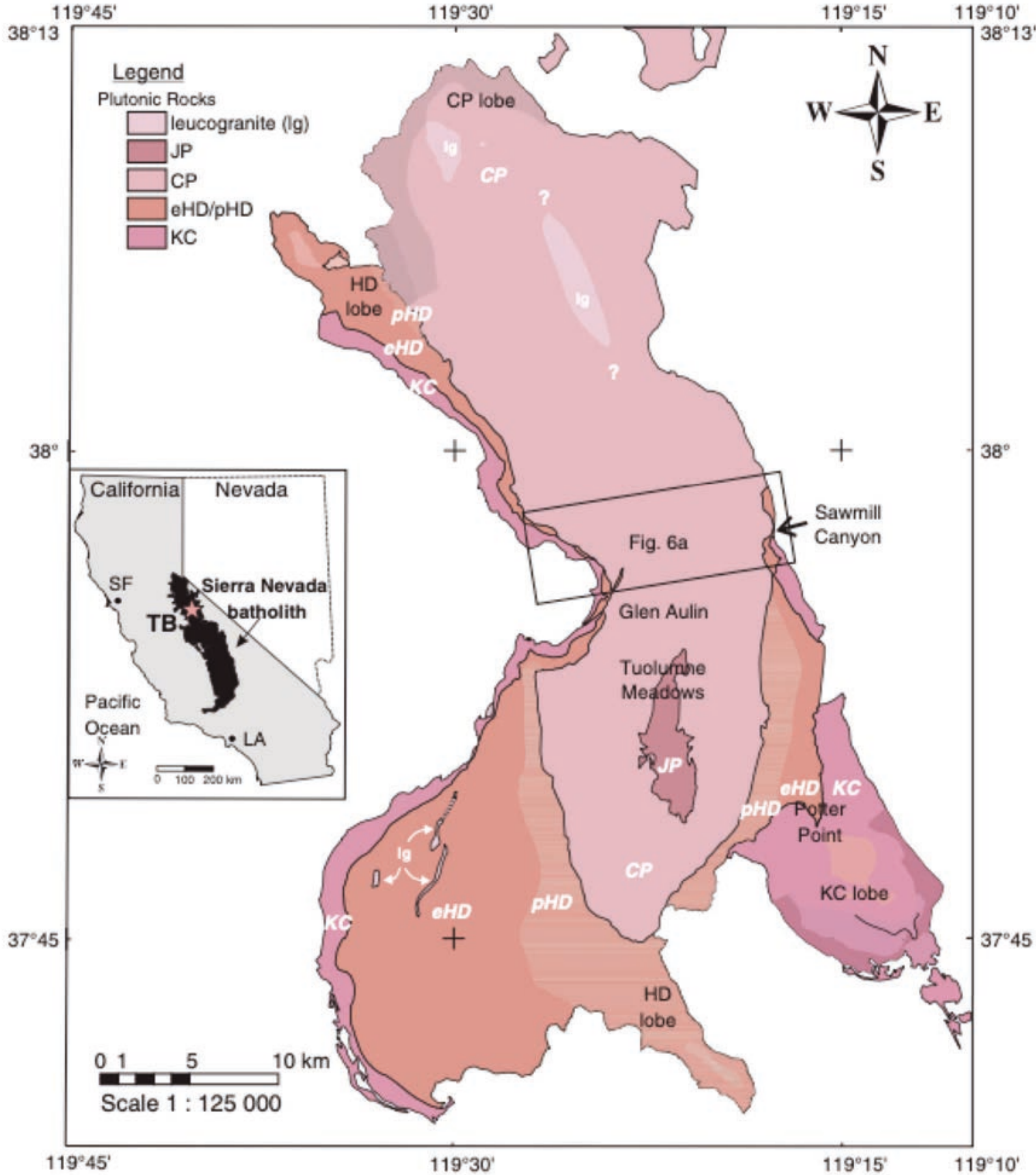

Figure 1. Geologic map of Tuolumne batholith and its host rocks (after Huber et al., 1989). Includes new mapping (by Paterson and colleagues) of much of the batholith at a scale of 1:24,000. Note the five main units in the central batholith and presence of additional internal zoning in the four lobes extending out from the units in the central batholith (after mapping by Memeti and colleagues). The structures discussed in this paper occur in all units and in lobes. Index map shows location of Tuolumne batholith (TB) in California. Box indicates location of Figure 6A. KC—Kuna Crest unit; CP—Cathedral Peak granodiorite; JP—Johnson granite porphyry; HD—Half Dome granodiorite (p is porphyritic, e is equigranular); SF—San Francisco; LA—Los Angeles.

Paterson (2009; Geosphere)

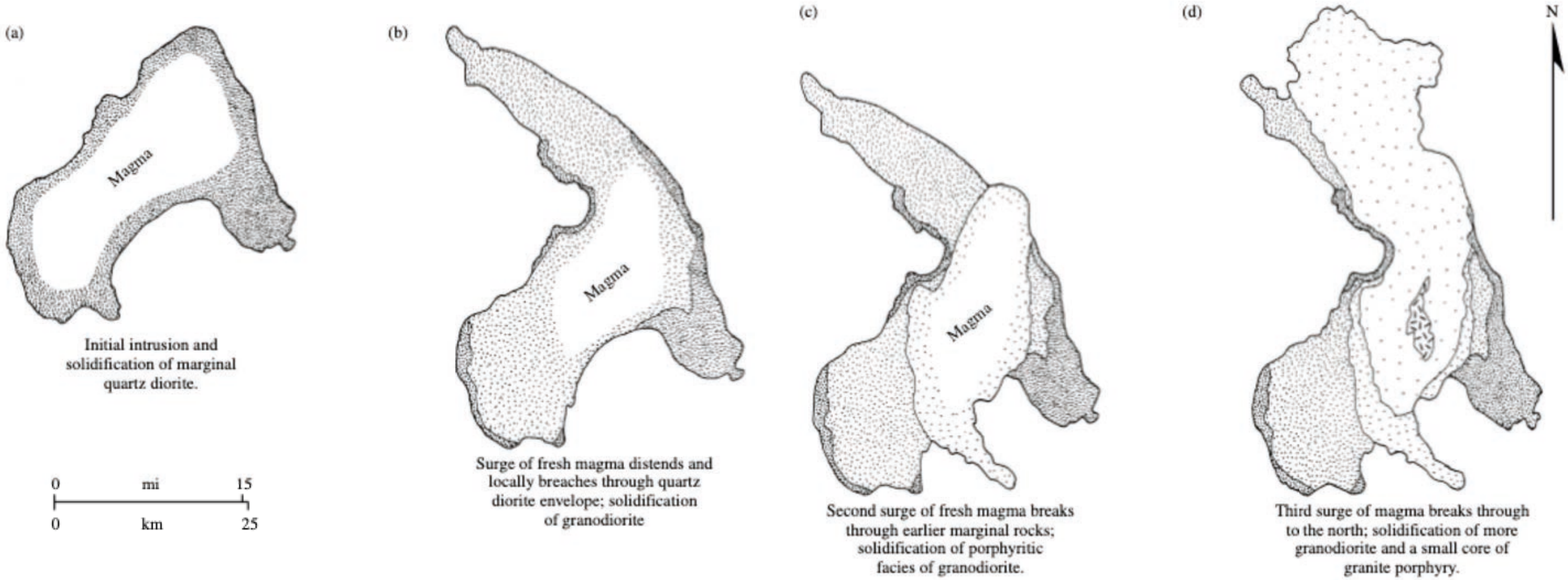

9.18 Evolution of the Tuolumne Intrusive Series, a compositionally **zoned pluton** within the Sierra Nevada batholith, California. Mantle-derived basalt magmas contaminated by increasing amounts of partial melts of the lower continental crust were intruded into the shallower crust over a time span of several million years (Kistler et al., 1986). See also Table 13.8. (a–d) Schematic sequence of events during growth of pluton. (e) Compositional variations along a west-east line across the pluton. (Redrawn from Bateman and Chappell, 1979.)

Best (2003)

Third surge of magma breaks through to the north; solidification of more granodiorite and a small core of granite porphyry.

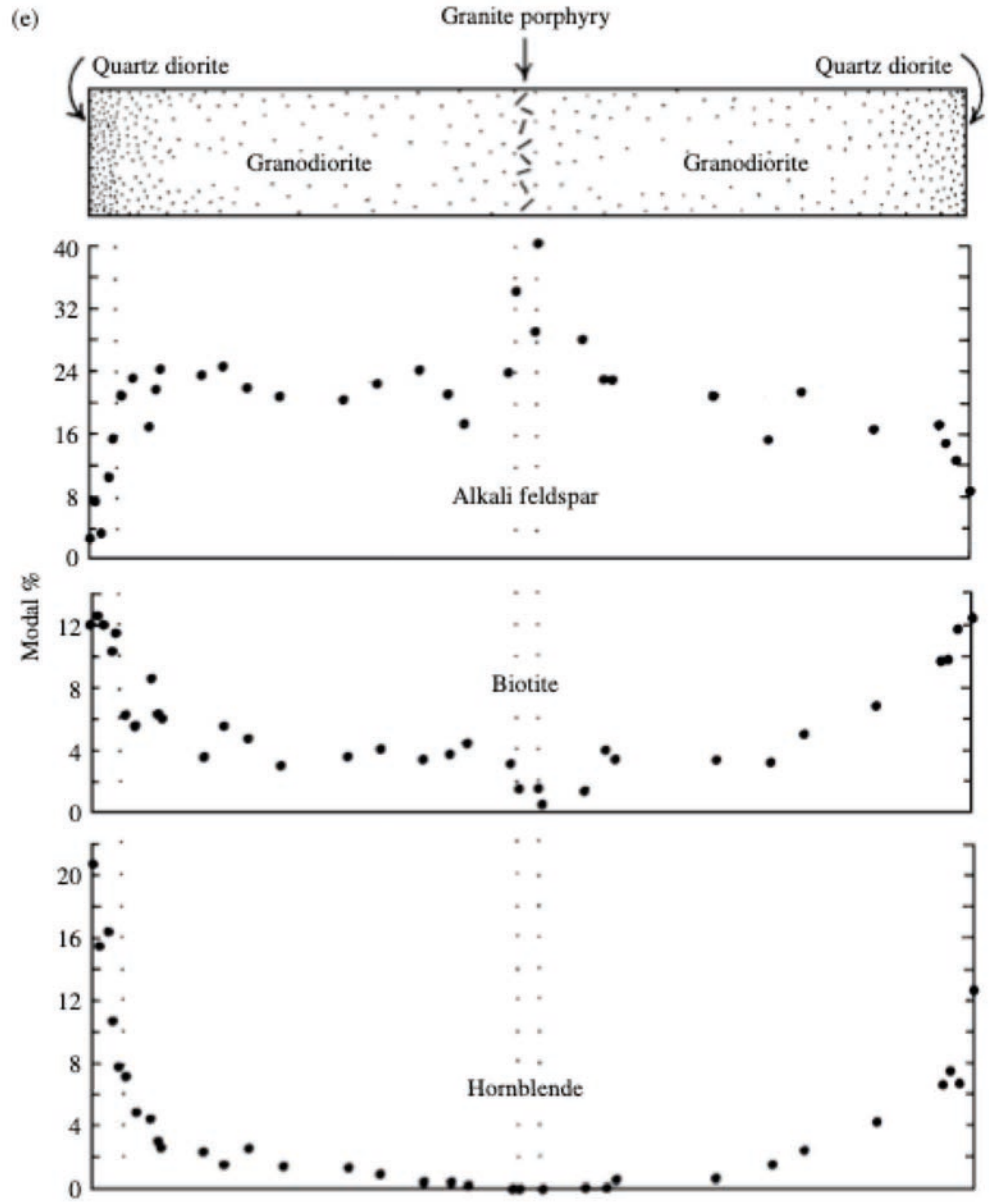

9.18 (*Continued*).

Best (2003)

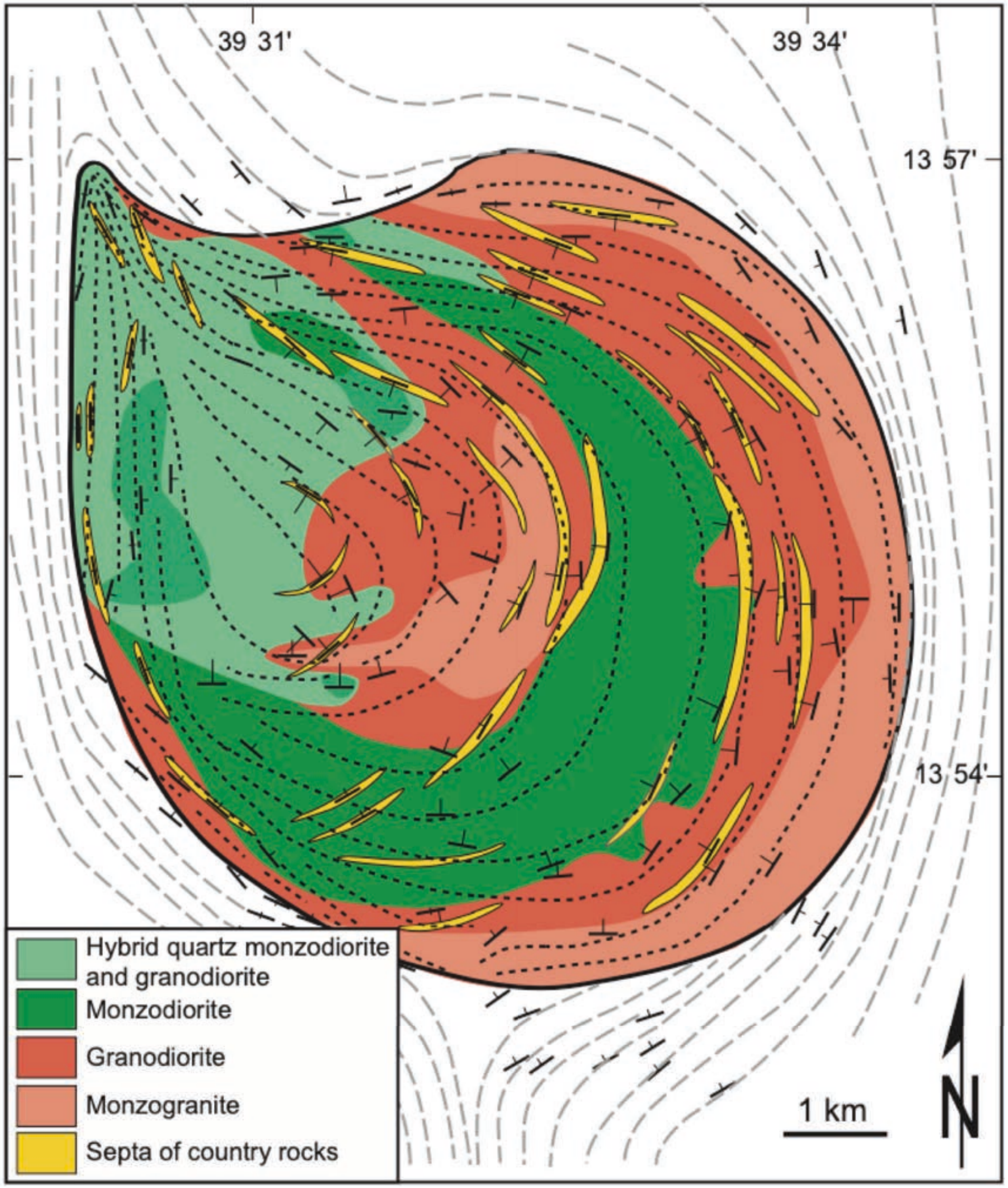

Figure 10. Geological map of the Negash pluton (northern Ethiopia) showing the shape and distribution of the country-rock septa; from Asrat et al. (2004).

Barbey (2009; Geol Belg)

Un **batolite** è un plutone, o più comunemente un gruppo di plutoni, che si estende generalmente dalla decina a molte centinaia di km.

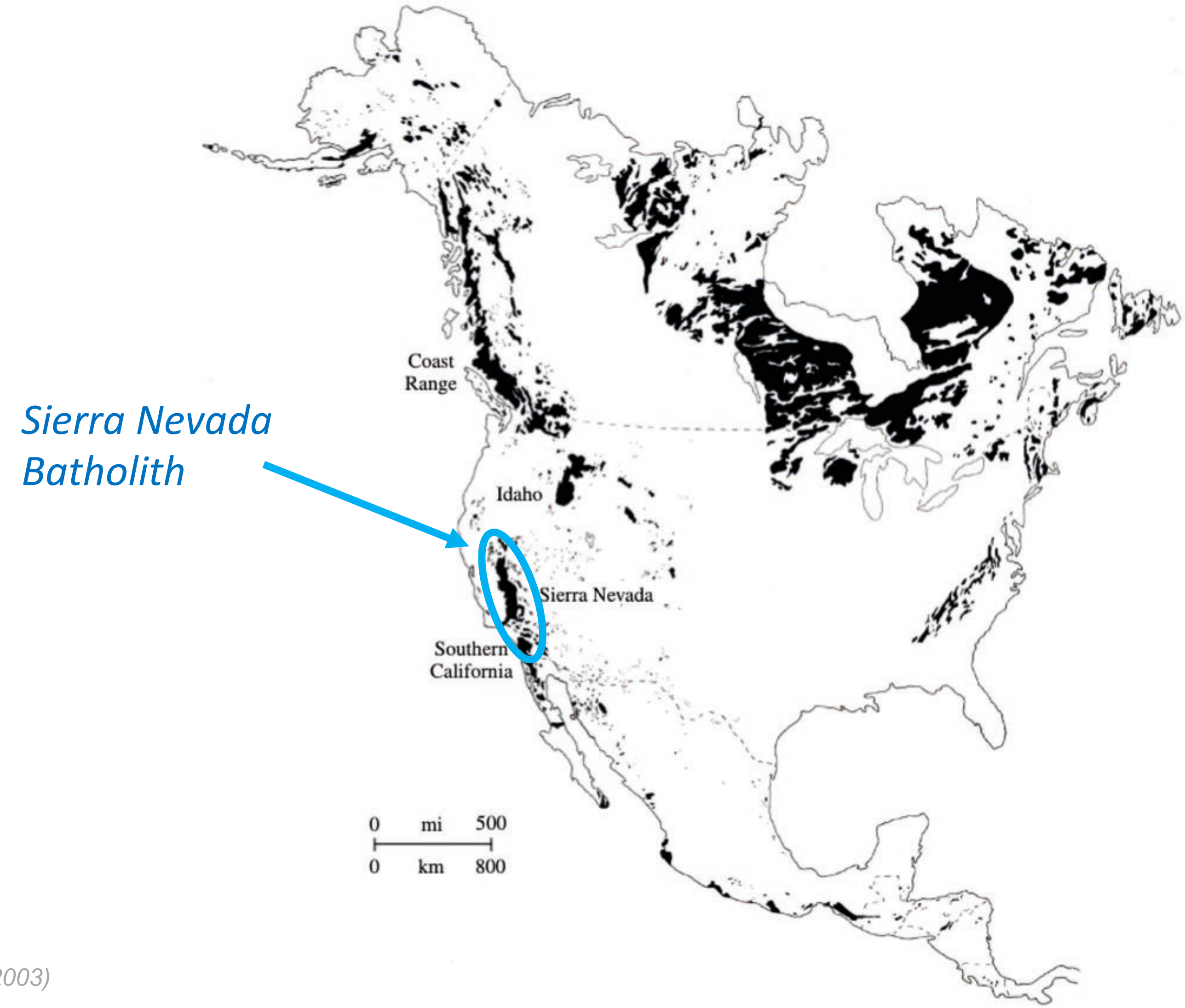

Best (2003)

9.16 Distribution of exposed granitic rocks in North America. Granitic rocks in Precambrian Canadian shield are generalized and include some metamorphic rocks. Rocks in the Appalachian orogen along the U.S. East Coast are mostly Paleozoic. Labeled **batholiths** along the west coast in the Cordilleran orogen are mostly Mesozoic. (Redrawn from the Tectonic Map of North America, U.S. Geological Survey.)

Un **batolite** è un plutone, o più comunemente un gruppo di plutoni, che si estende generalmente dalla decina a molte centinaia di km.

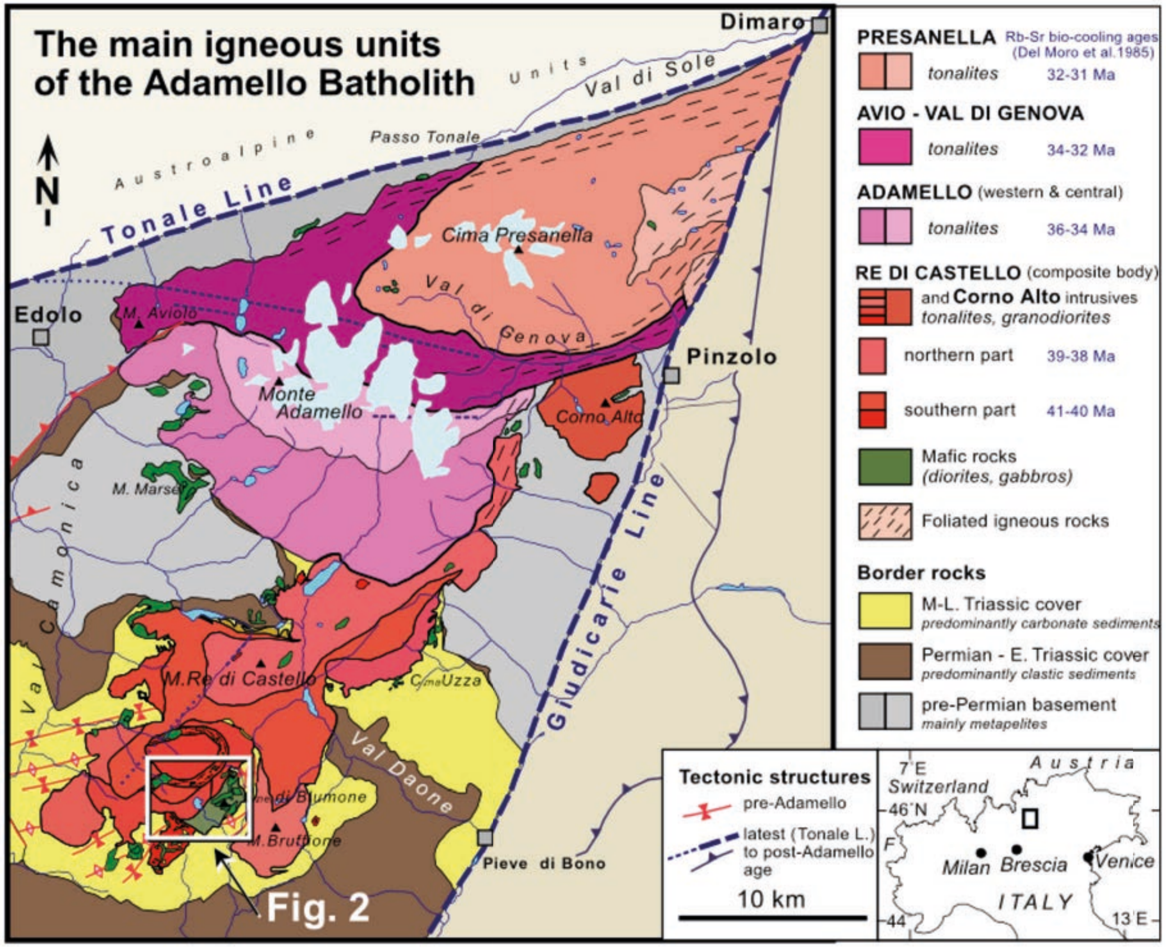

Fig. 1. Simplified geologic map of the Adamello batholith after Schaltegger et al. (2009), illustrating the approximate ages, lithologic characteristics, and designations of the main igneous units. See Schaltegger et al. (2009) for more detailed map and geochronology of the Re di Castello pluton. Location of the field site and Fig. 2 is outlined by the white box.

Schoene et al. (2012; EPSL)

(Adamello)

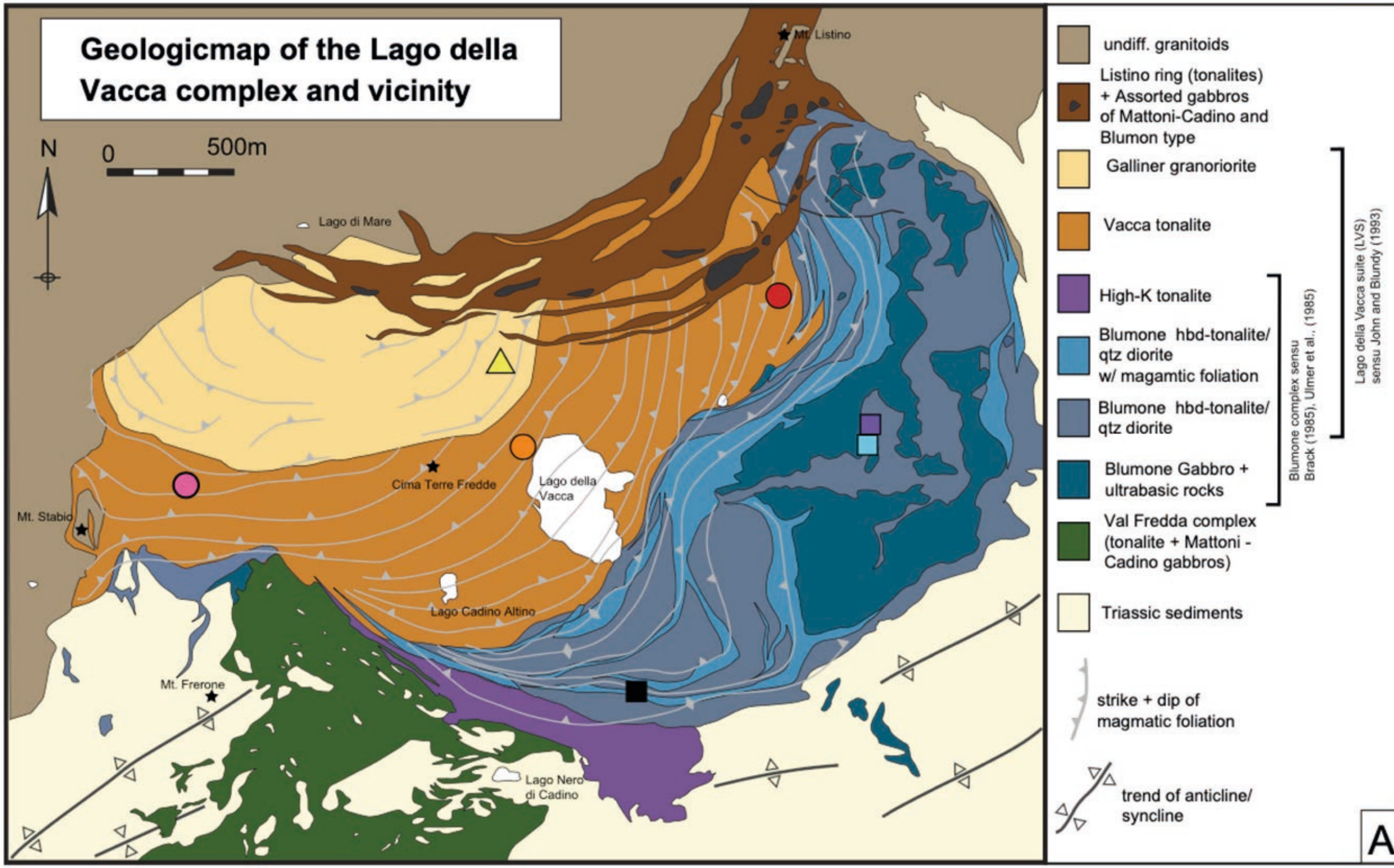

Schoene et al. (2012; EPSL)

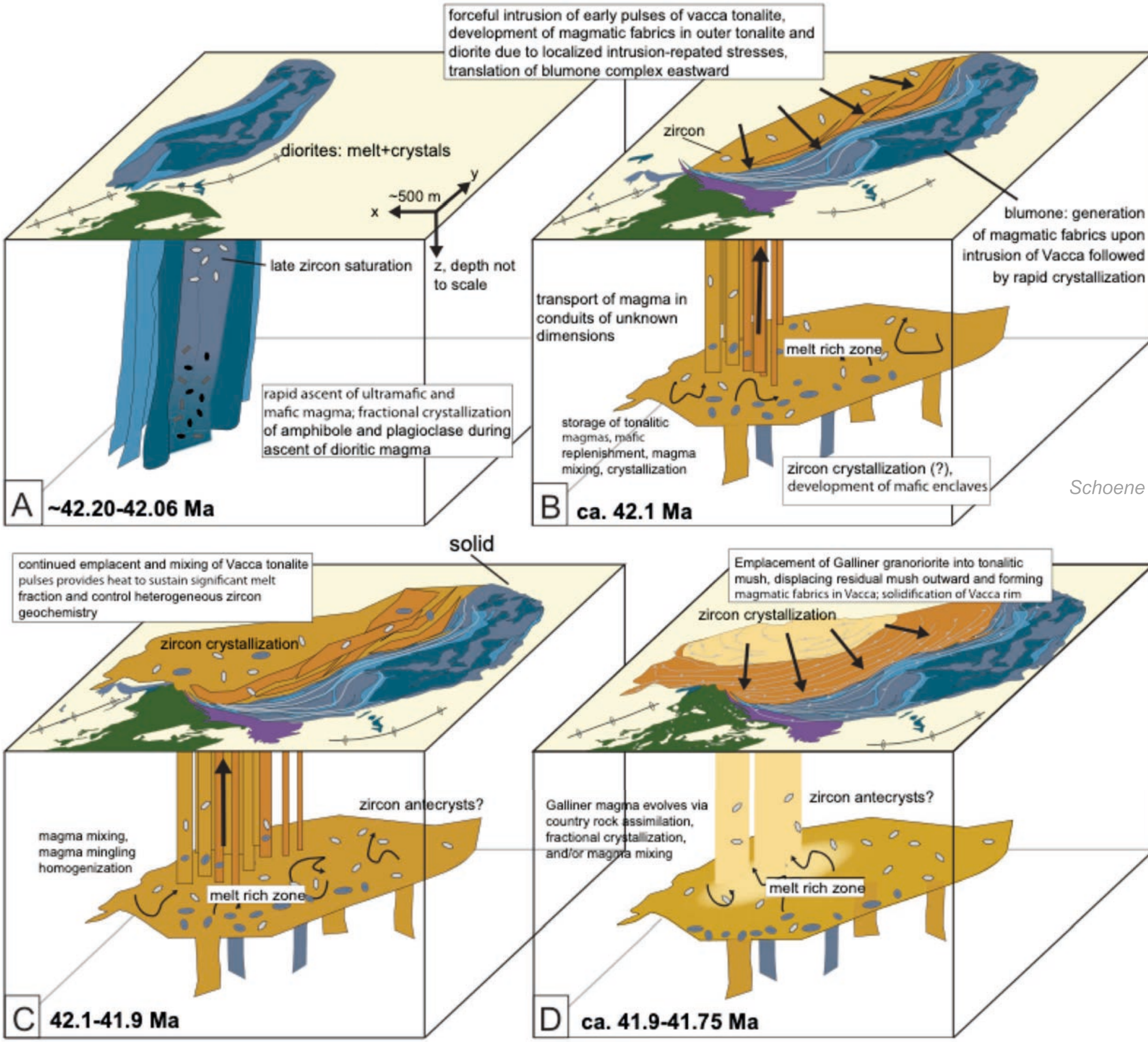

Schoene et al. (2012; EPSL)

Le intrusioni magmatiche possono essere eterogenee a tutte le scale.

Le micro- e le macro-strutture che le caratterizzano si formano dal contributo dei processi sia magmatici che tettonici. Queste strutture possono essere determinate tramite le relazioni di campo, la petrografia, la geochimica e la geologia strutturale.

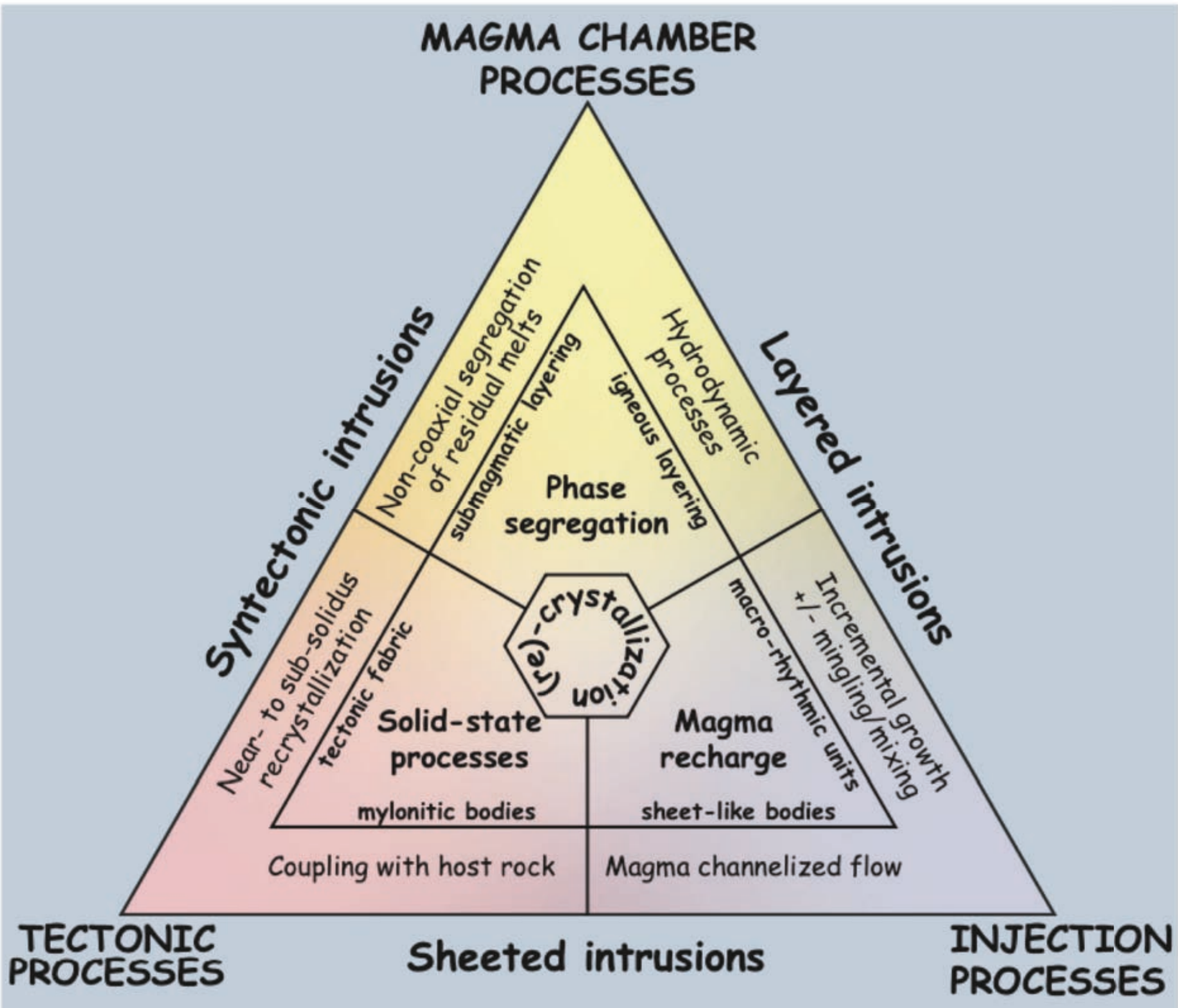

Barbey (2009; Geol Belg)

Barbey (2009; Geol Belg)

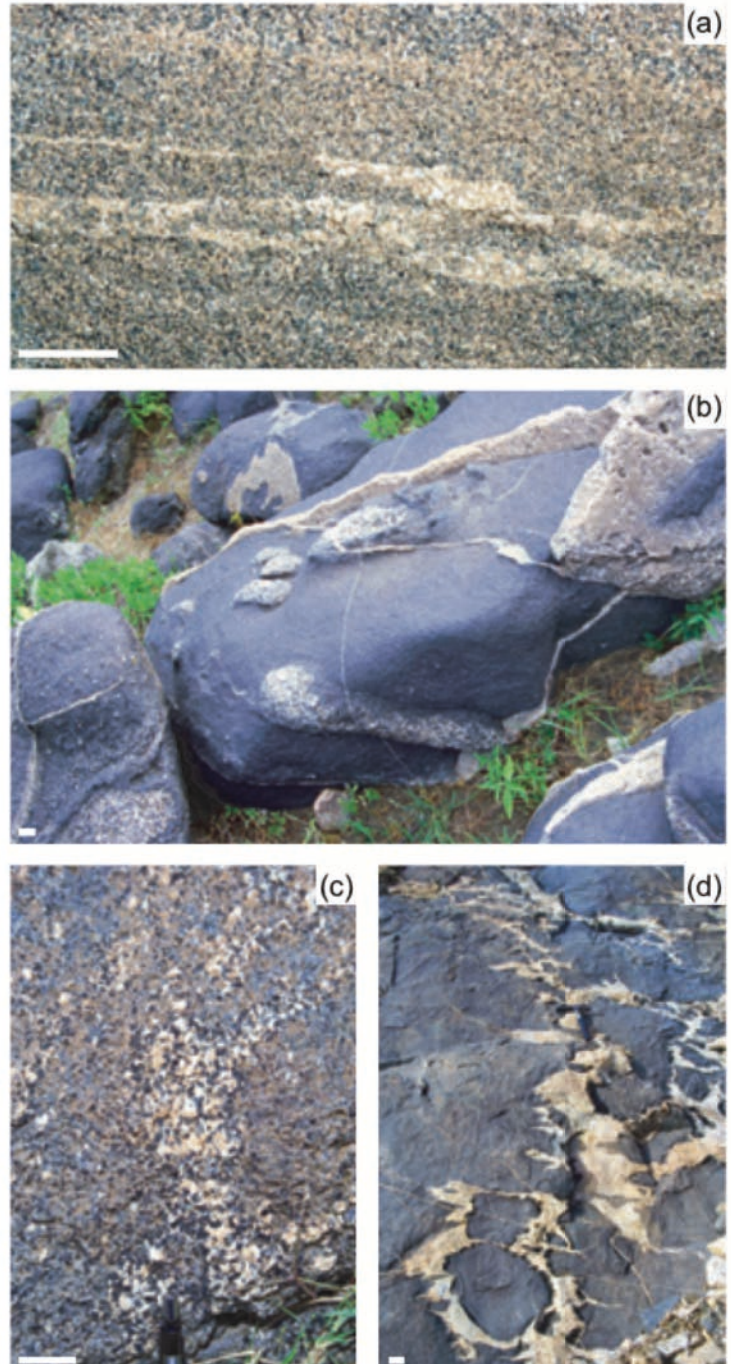

Figure 4. Granitic melt segregations in mafic-silicic layered intrusions. **(a)** Leucogranitic melt segregation layers parallel to igneous layering in granodiorite (Tarçouate pluton, Morocco; vertical cut; scale bar: 2 cm). **(b)** and **(c)** Granitic pipes and veins cutting through mafic layer (Negash pluton, Ethiopia; scale bar: 3 cm). **(d)** Mafic sheets crosscut by net-veining of differentiated granite (Tahala pluton, Morocco; plan view; scale bar: 10 cm).

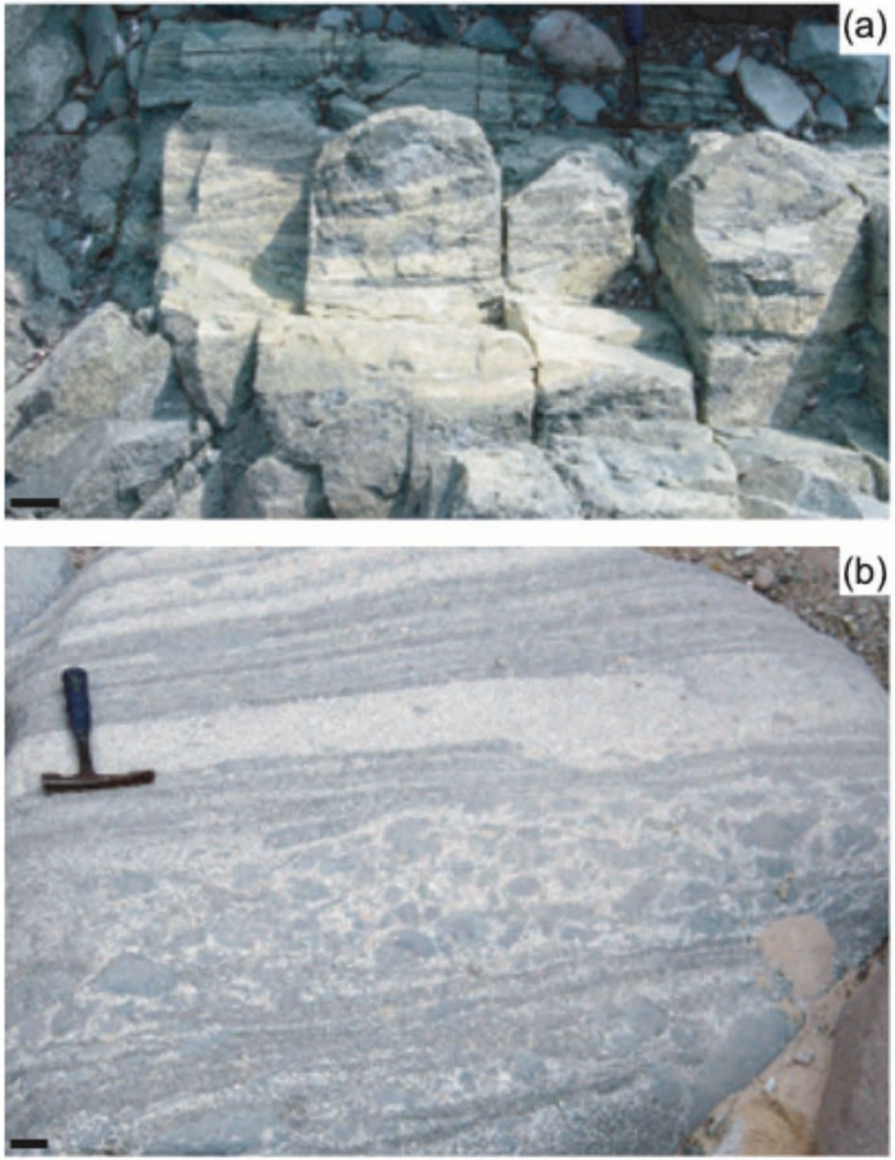

Figure 5. **(a)** Cross-stratifications in diorite (Coastal Batholith, Ilo, southern Peru; photograph T. Sempere). **(b)** Association of mafic enclaves and layering in granodiorite (Coastal Batholith, Huatiapa, southern Peru; photograph T. Sempere). **(c)** and **(d)** Schlieren in the Ploumanac'h massif (photographs F. Bussy). Scale bar: 10 cm.

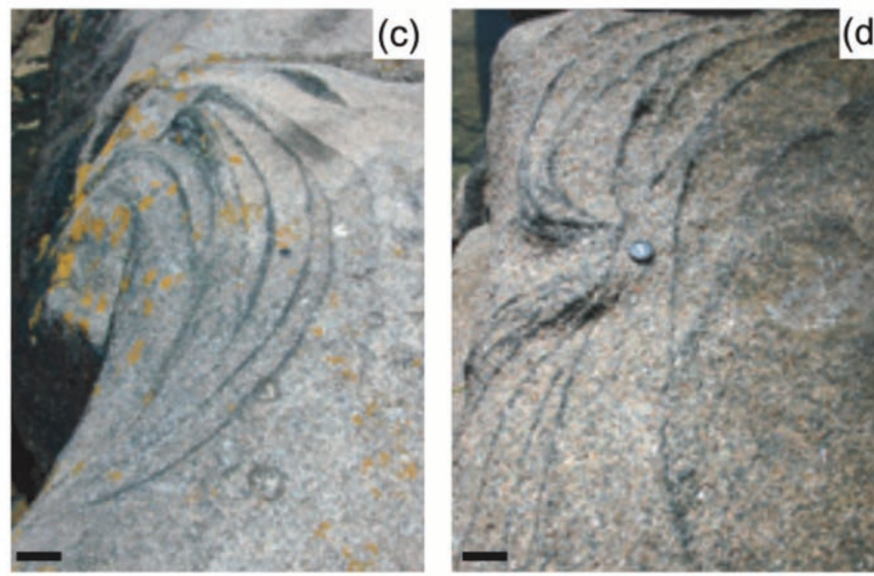

Barbey (2009; Geol Belg)

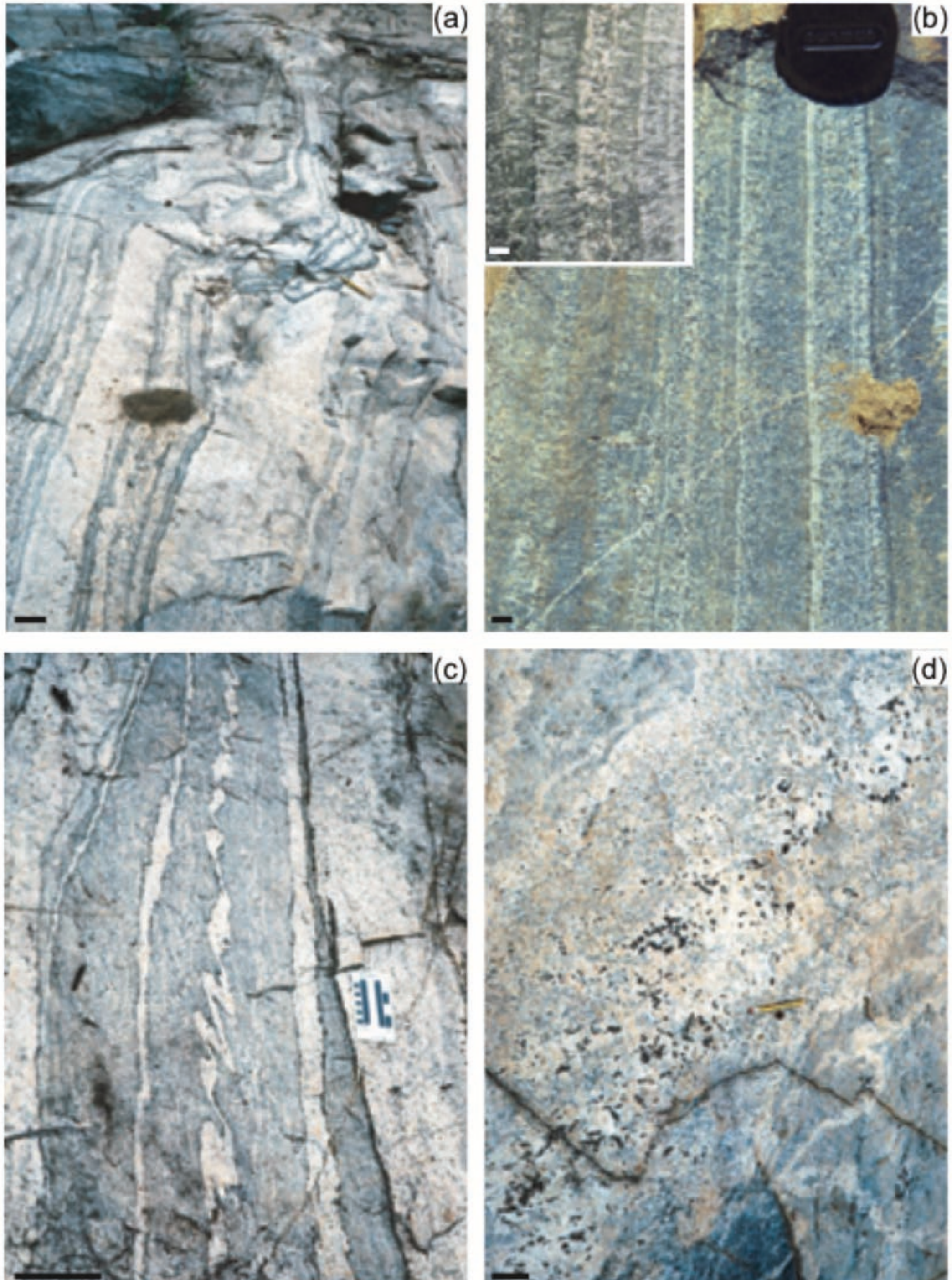

Figure 6. **(a)** Succession of paired isomodal biotite-rich and quartzofeldspathic layers. **(b)** Isomodal layering in a monzodiorite dyke associated with directional growth textures of feldspar (Tarçouate pluton, Morocco; scale bar: 1 cm). **(c)** Pegmatite veins parallel to the rhythmic layering; note the variable thickness of the veins and their distinct states of deformation indicating diachronic emplacement. **(d)**. Diffuse pegmatite patches delineating a loose layering structure. [(a), (c) and (d) Estrela Granite Complex, Carajàs Province, Brazil; scale bar = 10 cm].

Barbey (2009; Geol Belg)

Vinalhaven Intrusive Complex

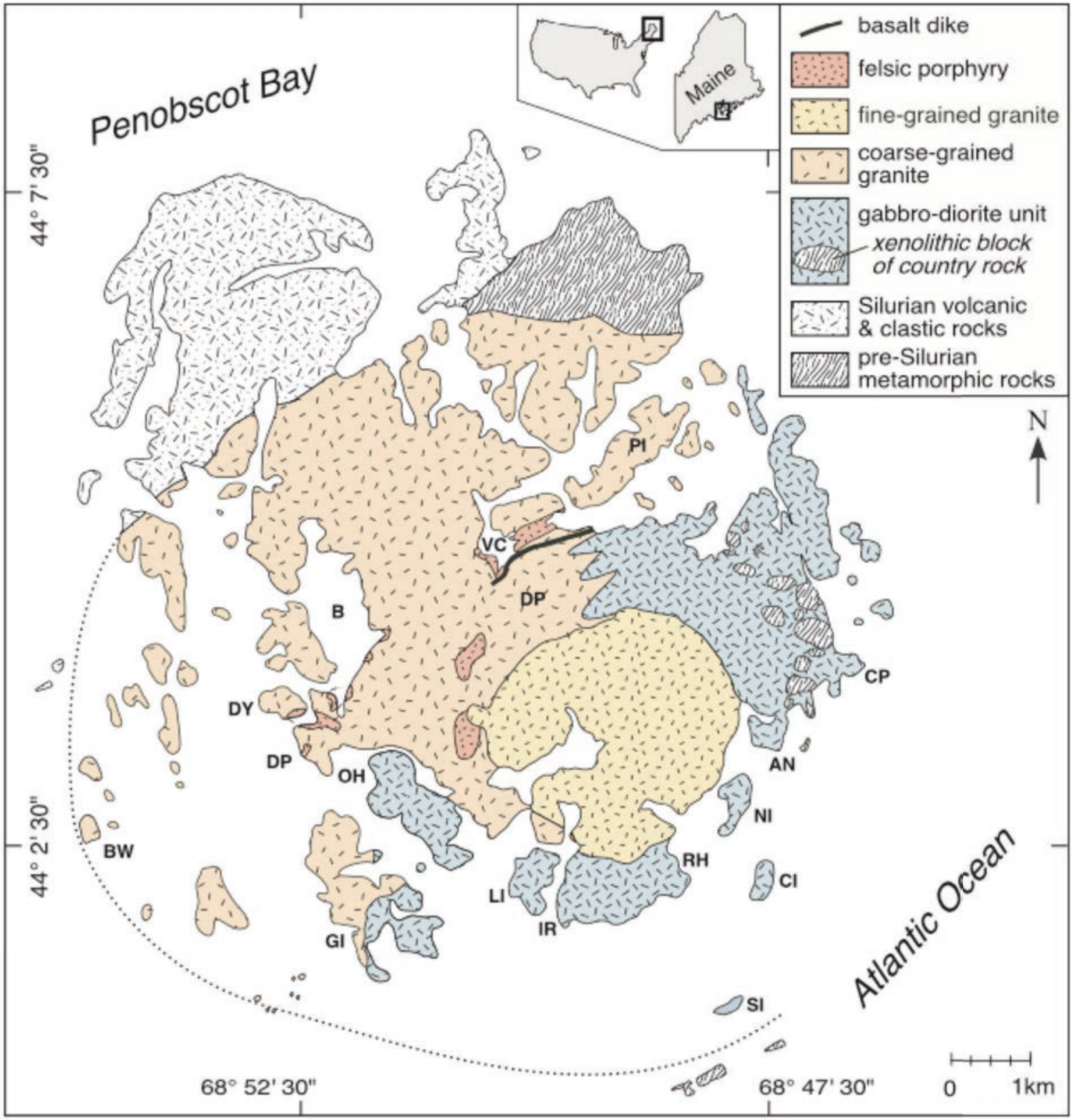

Fig. 1. Geological map of Vinalhaven Island. Pre-Silurian rocks exposed along the NE margin of the VIC are strongly foliated metamorphic rocks of the Calderwood Formation. Silurian, mostly unfoliated, rocks exposed along the coast include siliciclastic rocks of the Seal Cove Formation and volcanic and volcaniclastic rocks of the Vinalhaven rhyolite. Locations mentioned in the text: AN, Arey Neck; B, The Basin; BW, Big White Island; CI, Carvers Island; CN, Coombs Neck; CP, Calderwood Point; DP, Dog Point; DY, Dyer Island; GI, Greens Island; IR, Indian River; LI, Lanes Island; NI, Narrows Island; OH, Old Harbor; PI, Penobscot Island; RH, Roberts Harbor; SI, Sheep Island; VC, Vinal Cove. Modified after Gates (2001).

Wiebe & Hawkins (2012; J Pet)

Vinalhaven Intrusive Complex

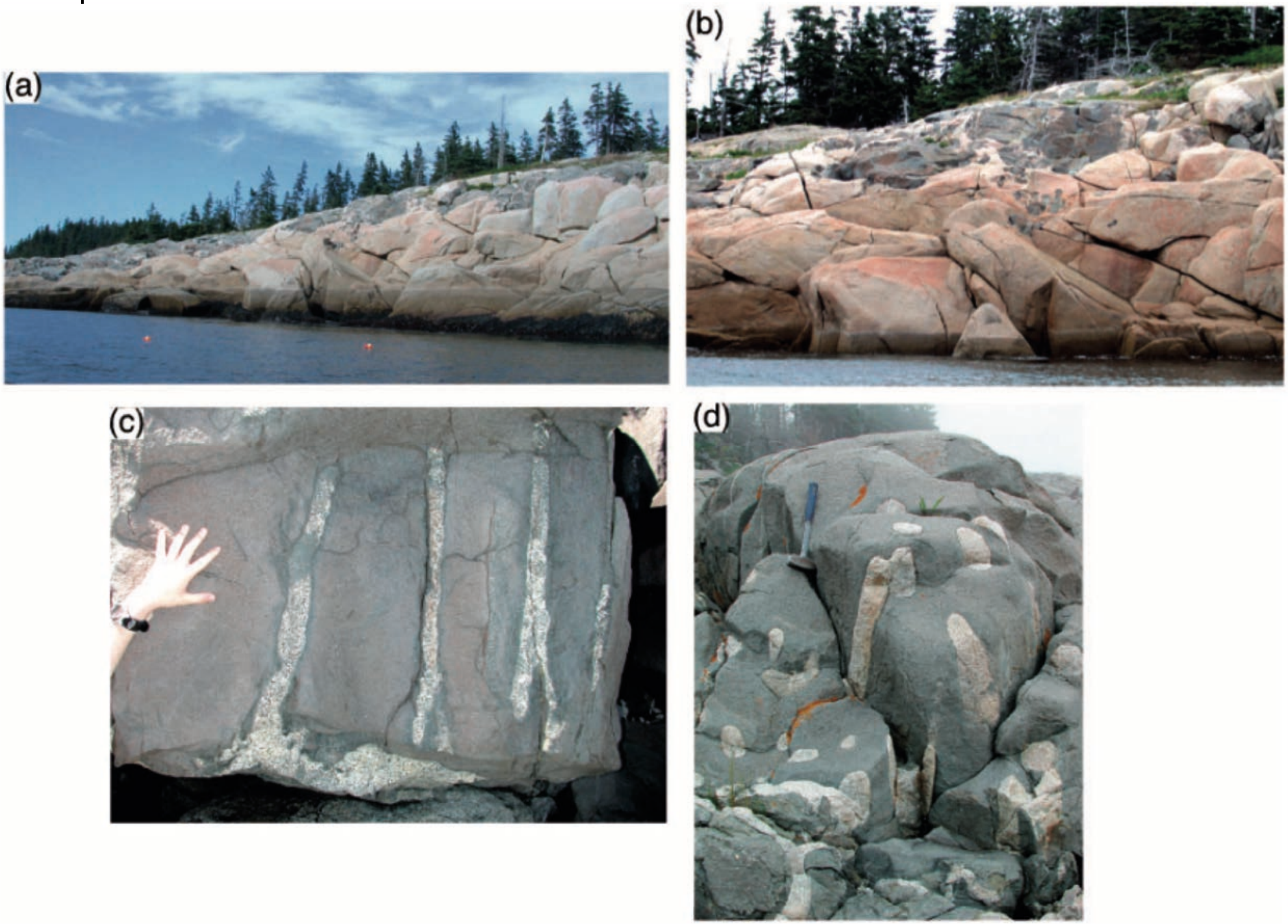

Wiebe & Hawkins (2012; J Pet)

Fig. 3. Field photographs of granitic diapiric bodies cutting the bases of macrorhythmic layers. (a) Distant view of base of gabbroic layer resting on coarse-grained granite. (b) Close-up view of the same contact, showing diapiric upwellings of granite extending more than 10 m upward into the gabbroic layer. (c) Thin felsic pipes connected to felsic top of underlying macrorhythmic layer. (d) Three-dimensional exposures of a cluster of coarse-grained granitic pipes in gabbro on Greens Island.

Vinalhaven Intrusive
Complex

Wiebe & Hawkins (2012; J Pet)

Fig. 6. Field photograph of a pillow mound from Old Harbor area (Fig. 1).

Vinalhaven Intrusive Complex

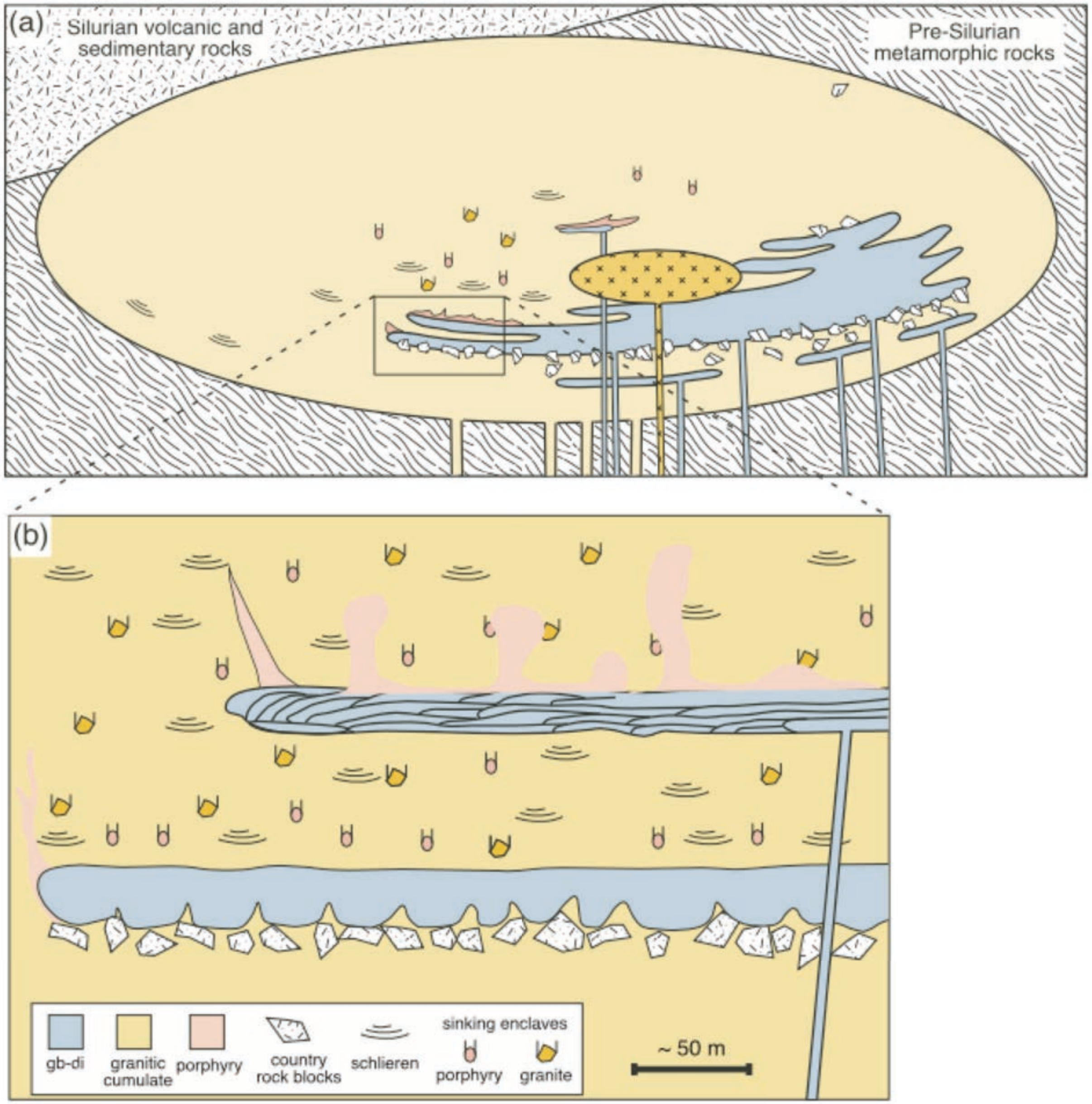

Fig. 16. (a) Schematic east–west oblique slice through the exposed part of the VIC (essentially the map viewed looking northward down the dip of the mafic sheets). It should be noted that the lower margin of the granite is not the base of the plutonic rocks, but only the southern margin of the exposed pluton. Mafic enclaves in granite below the exposed mafic rocks, gravity data and recycled zircons with ages that extend back to the age of volcanic rocks cut by the pluton roof (Hawkins *et al.*, 2009) require that a substantial volume of pluton must exist at greater depth. (b) Cross-section through the western terminations of the two gabbrodiorite sheets located at the southern end of Greens Island and at Old Harbor (GI and OH in Fig. 1). Gb-di, gabbrodiorite. (See text for details.)

Wiebe & Hawkins (2012; J Pet)

Le intrusioni magmatiche possono essere eterogenee a tutte le scale.

Le micro- e le macro-strutture che le caratterizzano si formano dal contributo dei processi sia magmatici che tettonici. Queste strutture possono essere determinate tramite le relazioni di campo, la petrografia, la geochimica e la geologia strutturale.

Vediamo l'esempio del batolite di Tuolumne (Sierra Nevada)

(tratto da Paterson et al. 2009)

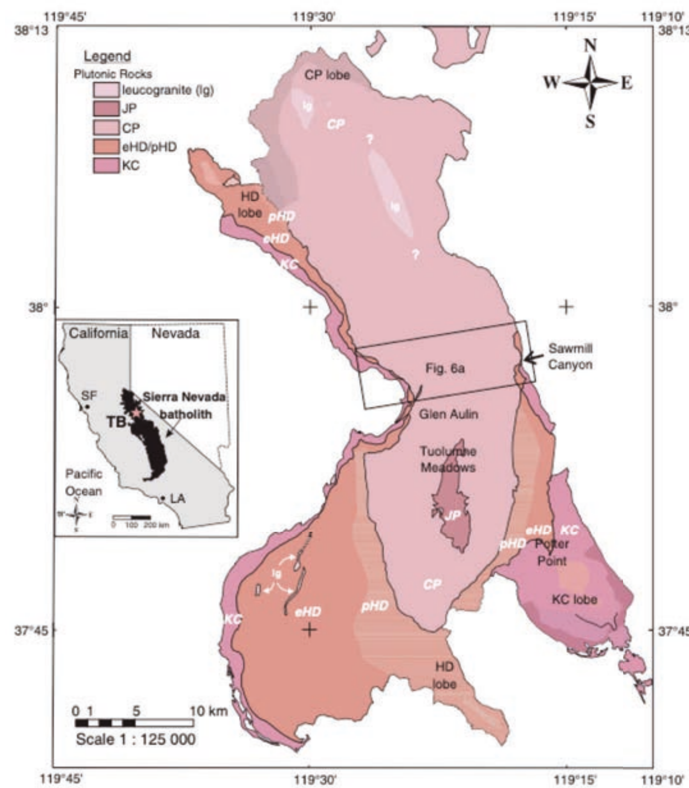

Figure 1. Geologic map of Tuolumne batholith and its host rocks (after Huber et al., 1989). Includes new mapping (by Paterson and colleagues) of much of the batholith at a scale of 1:24,000. Note the five main units in the central batholith and presence of additional internal zoning in the four lobes extending out from the units in the central batholith (after mapping by Memeti and colleagues). The structures discussed in this paper occur in all units and in lobes. Index map shows location of Tuolumne batholith (TB) in California. Box indicates location of Figure 6A. KC—Kuna Crest unit; CP—Cathedral Peak granodiorite; JP—Johnson granite porphyry; HD—Half Dome granodiorite (p is porphyritic, e is equigranular); SF—San Francisco; LA—Los Angeles.

Paterson et al. (2009; Geosphere)

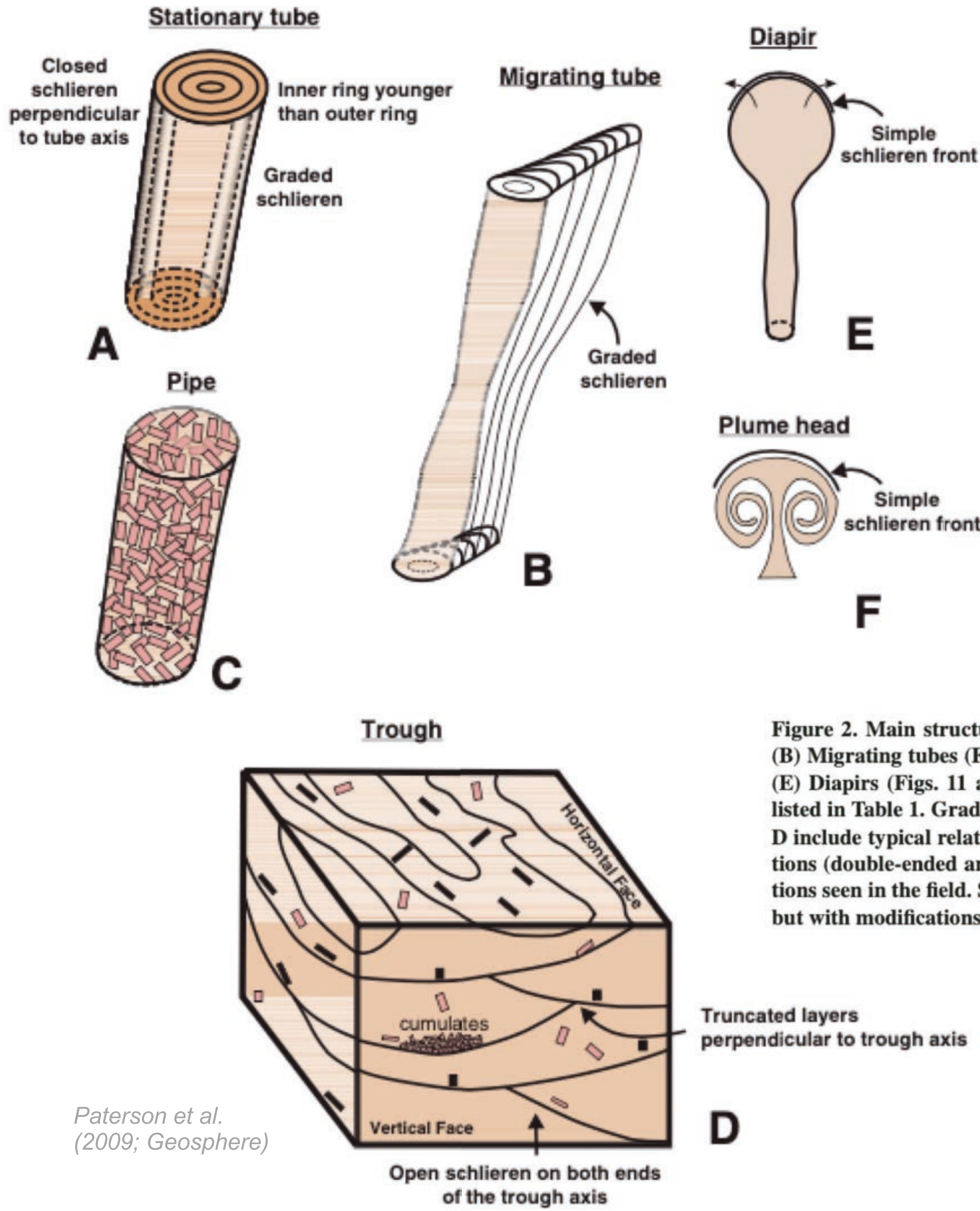

Paterson et al. (2009; Geosphere)

Schlieren (concentrazioni di materiale mafico all'interno di corpi granitici/granodioritici)

Figure 2. Main structures discussed in this paper. (A) Stationary tubes (Figs. 3 and 5A). (B) Migrating tubes (Figs. 4 and 5). (C) Pipes (Figs. 7 and 8). (D) Troughs (Figs. 9 and 10). (E) Diapirs (Figs. 11 and 12). (F) Plume heads (Fig. 13). The distinguishing features are listed in Table 1. Graded schlieren layers shown where developed in structures. Troughs in D include typical relationships between trough cutoffs, mineral fabrics, magma flow directions (double-ended arrow, as absolute flow direction is uncertain), and crystal accumulations seen in the field. Some drawings are influenced by diagrams in Weinberg et al. (2001), but with modifications.

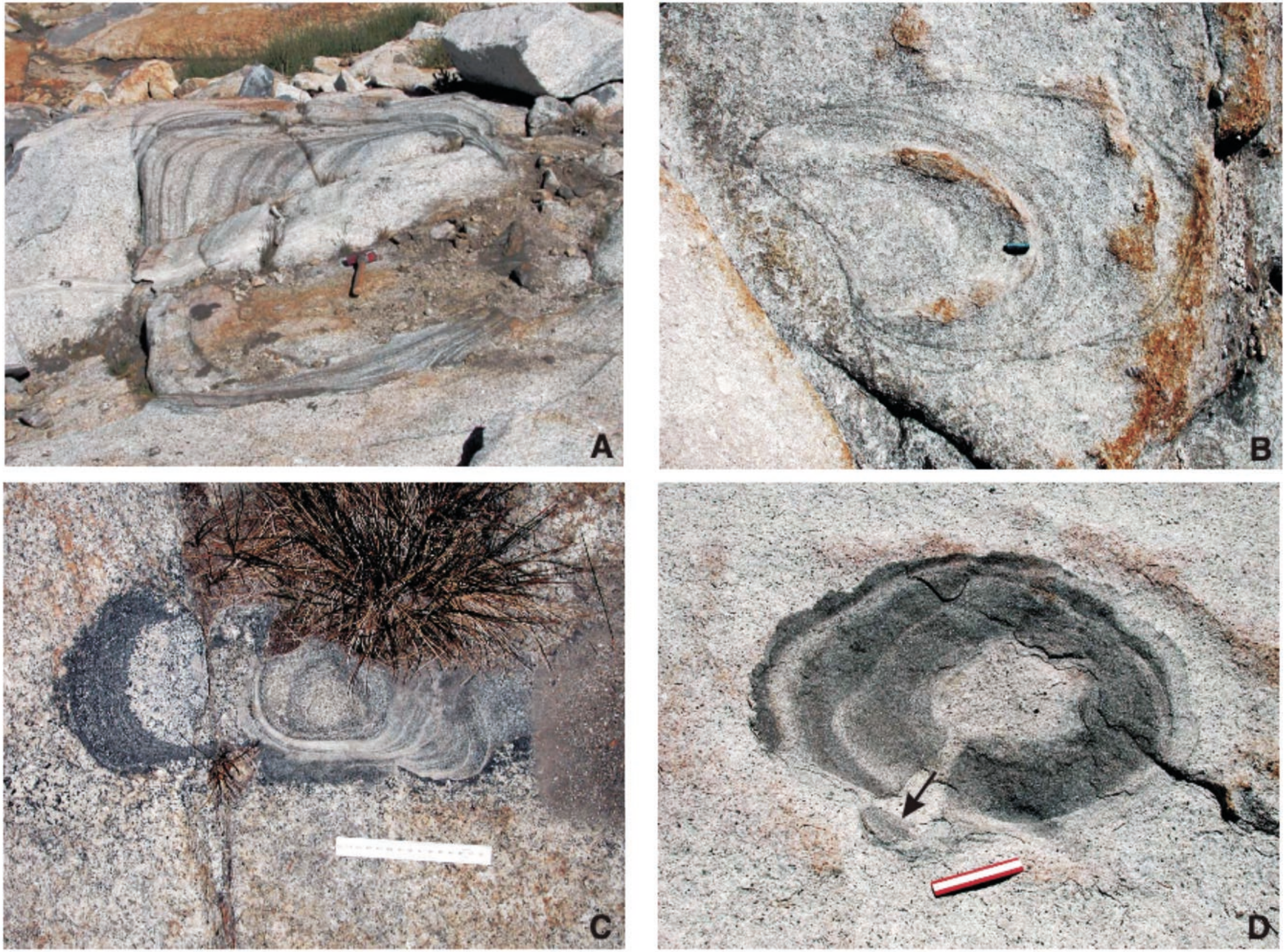

Figure 3. Photos of stationary (nonmigrating), steeply plunging tubes in the Tuolumne batholith (for other examples, see Weinberg et al., 2001; Žák and Klomínský, 2007). Crosscutting relationships between schlieren always indicate younging inward, that is, tube diameters decrease with time. (A) Equigranular Half Dome (HD) granodiorite in southern HD lobe; hammer for scale is ~25 cm. (B) Cathedral Peak granodiorite; 6.5 cm lip balm for scale. (C) HD granodiorite magmas with variable compositions and textures in Turner Lake granite host. Ruler for scale is 15 cm. (D) Mafic HD granodiorite magma in Turner Lake granite. Note how part of mafic tube margin was broken off and displaced outward (parallel to arrow) by magma from tube center. Ruler for scale is 15 cm.

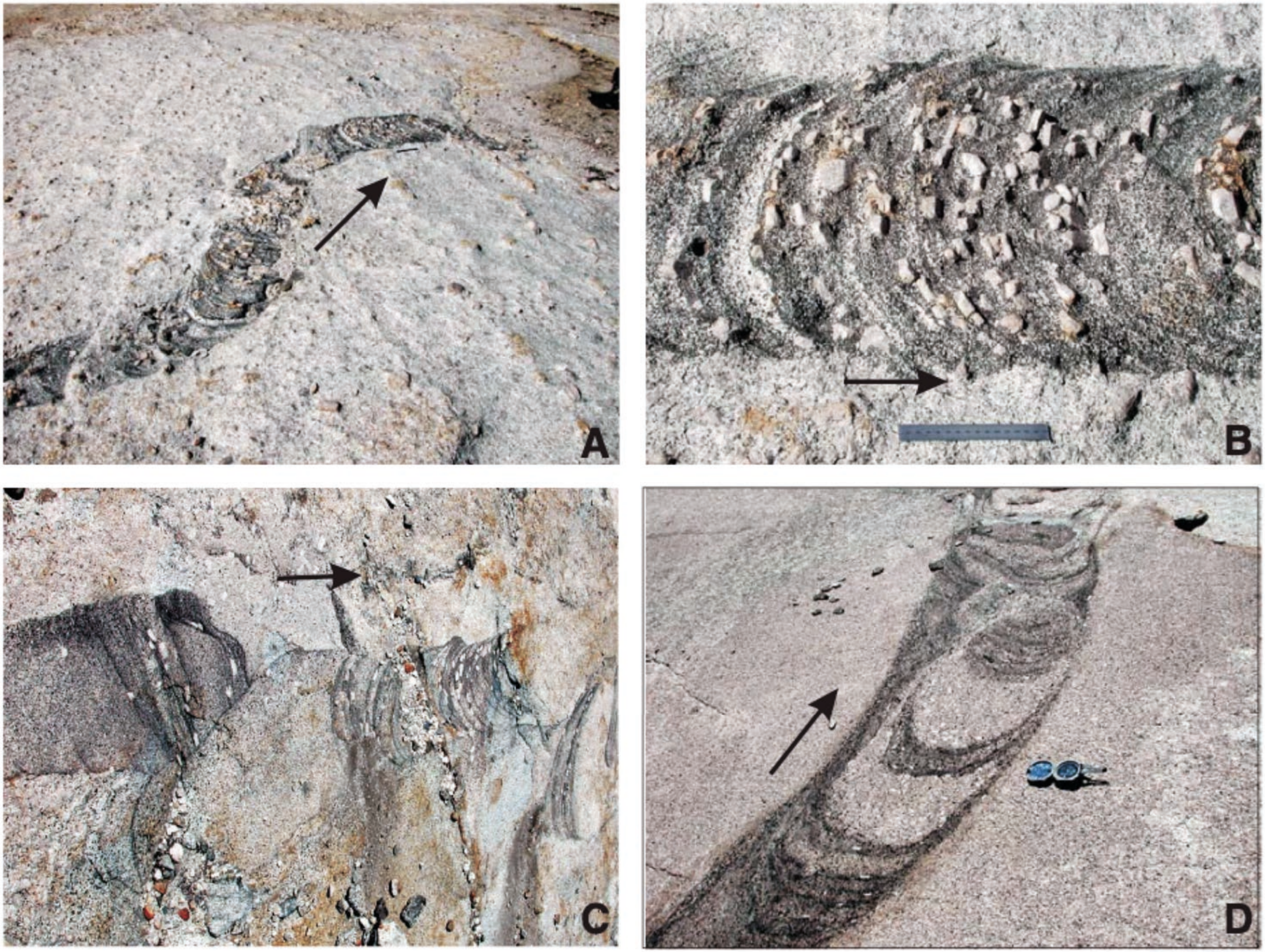
A
B
C
D

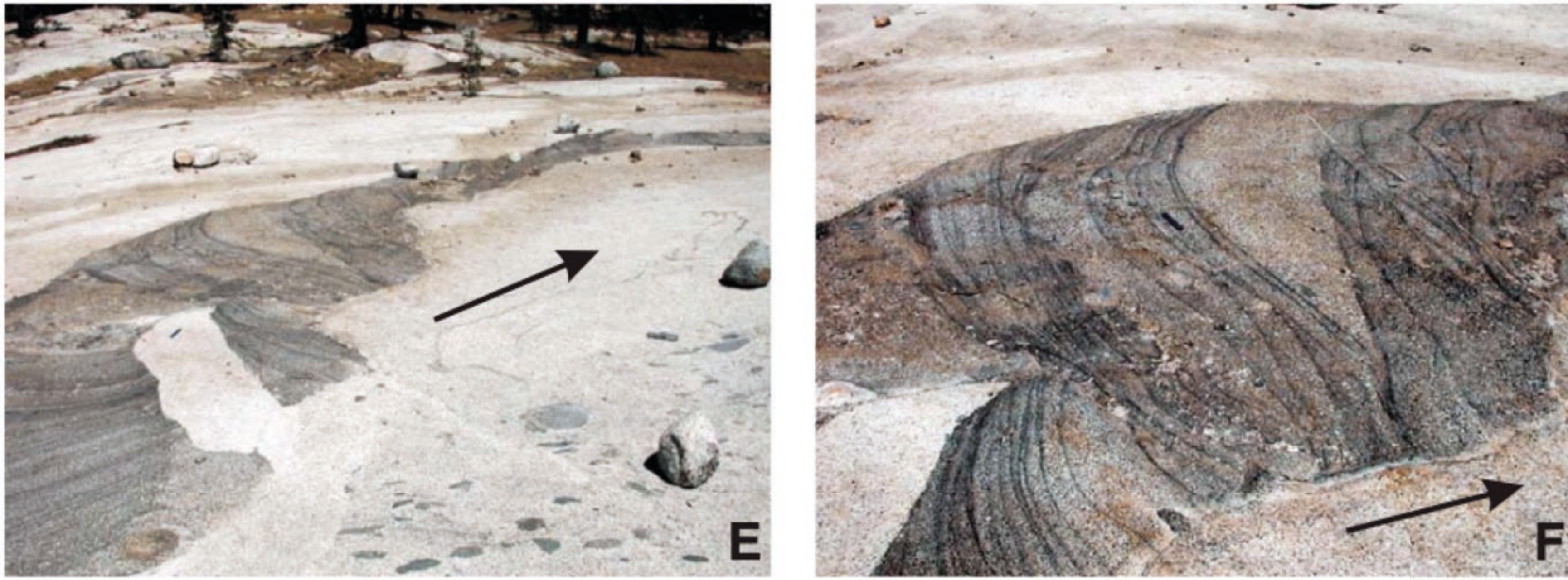

Figure 4. Photos of steeply plunging, migrating tubes in the Tuolumne batholith. Arrows show direction of migration. Ruler in photos A, B, E, and F is 15 cm. (A) Overview of migrating (southwest to northeast in photo) tube in the Cathedral Peak (CP) granodiorite; ruler near northeast end of tube for scale. (B) Close-up of one part of migrating tube shown in A. Note that the composition of felsic layers in tube are identical to host magma. (C) A row of several separate migrating tubes in the CP granodiorite. The first schlieren ring in one tube always truncates the last rings in the slightly older tube. All migrated in the same direction (left to right in photo). Some layers in tubes have K-feldspar megacrysts, others do not. Photo ~3 meter across. (D) Fairly mafic layers bounding migrating tube in the Half Dome granodiorite. Tube walls interdigitate with host magma and some rings in tube have field characteristics identical to those in the host granodiorite. Brunton compass for scale. (E) Migrating tube in transition zone between Half Dome and Kuna Crest unit granodiorites near Potter Point, Lyell Canyon. Tube is reintruded by host magma and decreases its diameter as it youngs (parallel to arrow) toward top of photo. Ruler is in region of reintrusion. (F) Close-up of one part of tube in E showing heterogeneous compositions and truncation of tube walls indicating younging (migration of) tube to right in photo (parallel to arrow).

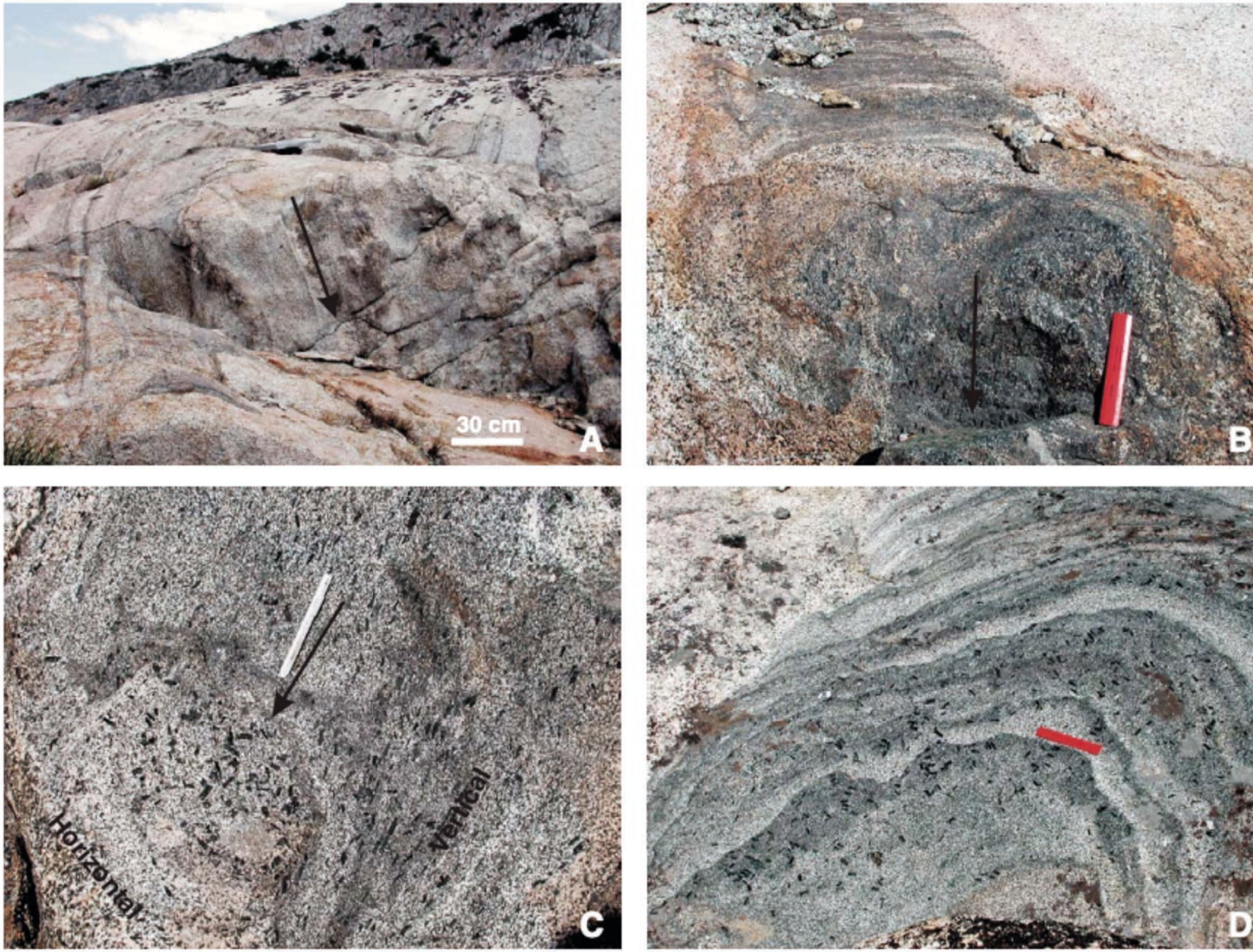

Figure 5. Three-dimensional view of tubes showing subvertical schlieren-bounded walls and steeply plunging tube axes (parallel to black arrows). (A) Cathedral Peak granodiorite. (B) Half Dome (HD) granodiorite; 15 cm ruler against vertical surface for scale. Subhorizontal surfaces at top of photo and below ruler. (C) HD granodiorite; 15 cm ruler against vertical surface for scale. Subhorizontal surface immediately below ruler with closed schlieren layers. (D) Hornblende phenocrysts in subhorizontal migrating tube in HD granodiorite. A few hornblendes are aligned parallel to schlieren layers, but many define an overprinting fabric or at high angles, as predicted by mineral tumbling experiments (Ildefonse et al., 1997); 15 cm ruler for scale. Note vertical mineral lineation defined by euhedral hornblendes in B and C and that these same hornblendes are more random or aligned parallel to schlieren layers in the subhorizontal surfaces in B–D. Also note that more leucocratic layers often are identical to and/or continuous with host granodiorites.

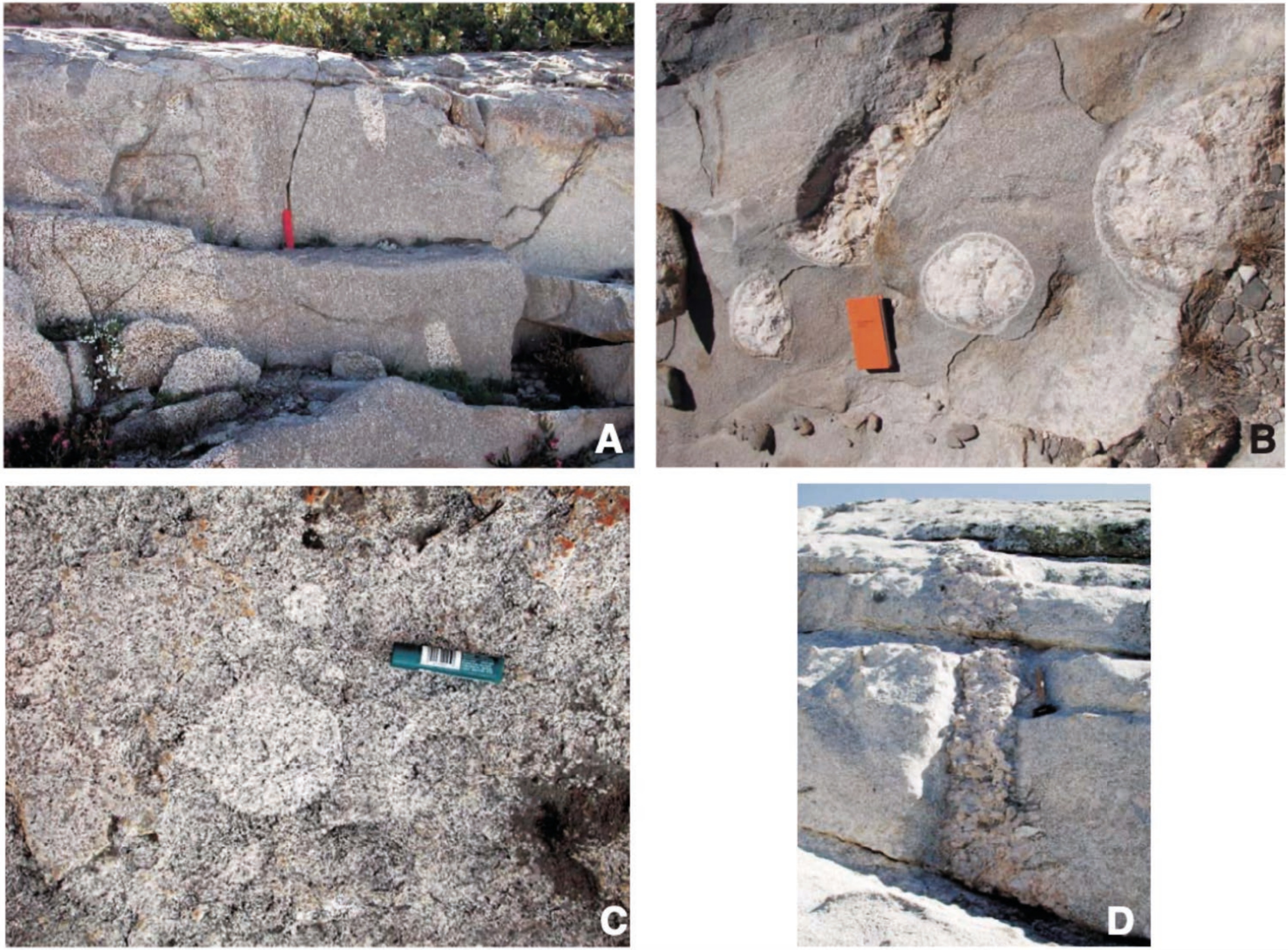
A
B
C
D

Figure 7. Photos of pipes. (A) Vertical surface through granodiorite pipes in quartz diorite sheets in Kuna Crest unit; 15 cm ruler for scale. (B) Subhorizontal surface through the pipes in A; 15 cm ruler for scale. Note that all pipes are roughly subvertical even in cases where the mafic layering is also steeply dipping (in contrast to Wiebe and Collins, 1998). (C) Horizontal surface through a number of small leucocratic granite pipes in Johnson granite porphyry; 6.5 cm lip balm for scale. (D) Vertical surface through cylindrical pipe K-feldspar megacryst–rich pipes (typically consisting of 60%–80% megacrysts by volume); 25 cm hammer for scale. A minor amount of biotite accumulation occurs along the pipe walls. (E) Closeup of one margin of a K-feldspar megacryst–rich pipes (typically consisting of 60%–80% megacrysts by volume) in the Cathedral Peak granodiorite. Thin schlieren along margin; 6.5 cm lip balm for scale. (F) Vertical surface through funnel-shaped pipe. Top of pipe is ~1 m across.

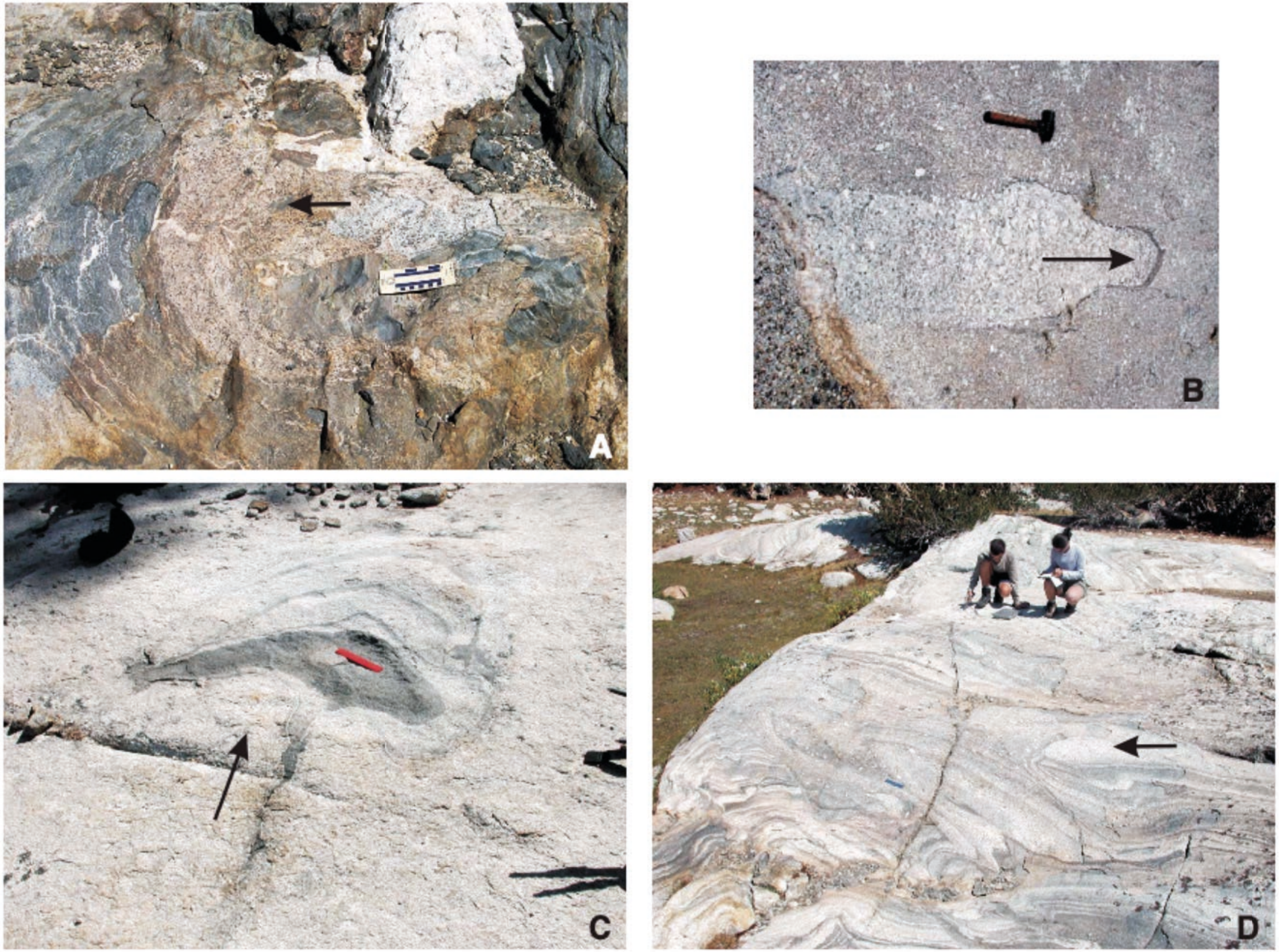

Figure 11. Photos of local diapirs with arrows showing inferred movement direction. (A) Mushroom-shaped diapir of Kuna Crest unit granodiorite in Sawmill Canyon pushing metavolcanic host rocks laterally away from the eastern margin of the Tuolumne batholith; 10 cm ruler for scale. (B) K-feldspar megacryst–rich diapir in Cathedral Peak granodiorite unit. Note accumulation of mafic minerals (mainly biotite and accessories) at the top of diapir; 25 cm hammer for scale. (C) Laterally moving diapir of quartz diorite in transitional phase of the Half Dome (HD) granodiorite; 15 cm ruler for scale. (D) Obliquely moving diapir of K-feldspar megacryst–bearing HD granodiorite, Sawmill Canyon area, moving into and deflecting schlieren layers in magmatic troughs.

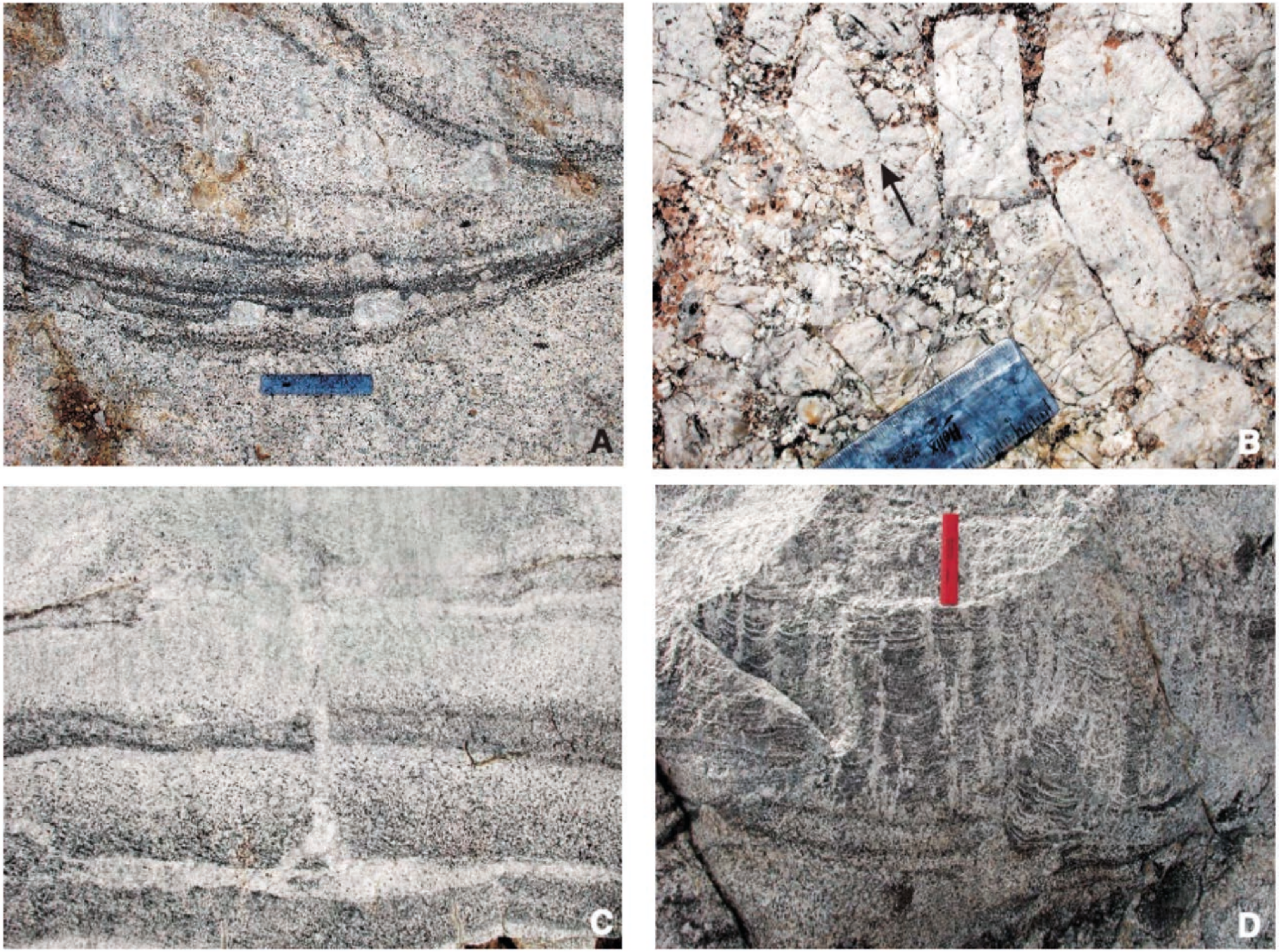

Figure 16. Photos of evidence of compaction during filter pressing associated with structures discussed in this paper. (A) Schlieren indented by K-feldspar megacrysts in trough in Cathedral Peak granodiorite (CP); 15 cm ruler for scale. (B) Closely packed and sometimes touching K-feldspar megacrysts in pipe in CP. Note that the touching megacrysts sometimes indent and truncate zoning in others (e.g., in front of black arrow), indicating compaction and likely contact melting (e.g., Park and Means, 1996; Paterson et al., 2005). End of 15 cm ruler for scale. (C) Layered mafic and felsic schlieren with vein of felsic material draining from a felsic layer through the overlying layers. Width of bottom of photo is ~0.5 m. (D) Dish and pillar–like structures (see text) formed as felsic melts rose through thin mafic layers, during which the rise of melts bent the mafic layers into small dish-shaped segments; 15 cm ruler for scale.